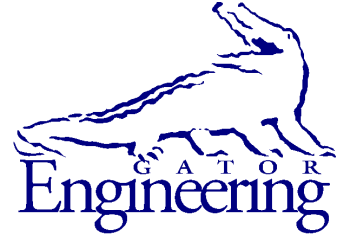**University of Florida**
Civil and Coastal Engineering

University of Florida
Civil and Coastal Engineering

UF

Final Report   **March 2013**

END REGION DETAILING OF PRETENSIONED CONCRETE BRIDGE GIRDERS

Principal investigator:
H. R. Hamilton

Co-Principal investigator:
Gary R. Consolazio

Research assistant:
Brandon E. Ross

Department of Civil and Coastal Engineering
University of Florida
P.O. Box 116580
Gainesville, Florida 32611

DISCLAIMER

The opinions, findings, and conclusions expressed in this publication are those of the authors and not necessarily those of the State of Florida Department of Transportation.

SI* (MODERN METRIC) CONVERSION FACTORS
APPROXIMATE CONVERSIONS *TO* SI UNITS

SYMBOL	WHEN YOU KNOW	MULTIPLY BY	TO FIND	SYMBOL
LENGTH				
in	inches	25.4	millimeters	mm
ft	feet	0.305	meters	m
yd	yards	0.914	meters	m
mi	miles	1.61	kilometers	km
AREA				
in^2	square inches	645.2	square millimeters	mm^2
ft^2	square feet	0.093	square meters	m^2
yd^2	square yard	0.836	square meters	m^2
ac	acres	0.405	hectares	ha
mi^2	square miles	2.59	square kilometers	km^2
VOLUME				
fl oz	fluid ounces	29.57	milliliters	mL
gal	gallons	3.785	liters	L
ft^3	cubic feet	0.028	cubic meters	m^3
yd^3	cubic yards	0.765	cubic meters	m^3
NOTE: volumes greater than 1000 L shall be shown in m^3				
MASS				
oz	ounces	28.35	grams	g
lb	pounds	0.454	kilograms	kg
T	short tons (2000 lb)	0.907	megagrams	Mg (or "t")
TEMPERATURE (exact degrees)				
°F	Fahrenheit	5(F-32)/9 or (F-32)/1.8	Celsius	°C
ILLUMINATION				
fc	foot-candles	10.76	lux	lx
fl	foot-Lamberts	3.426	candela/m^2	cd/m^2
FORCE and PRESSURE or STRESS				
kip	1000 pound force	4.45	kilonewtons	kN
lbf	pound force	4.45	newtons	N
lbf/in^2	pound force per square	6.89	kilopascals	kPa

*SI is the symbol for the International System of Units. Appropriate rounding should be made to comply with Section 4 of ASTM E380.

SI* (MODERN METRIC) CONVERSION FACTORS

APPROXIMATE CONVERSIONS *FROM* SI UNITS

SYMBOL	WHEN YOU KNOW	MULTIPLY BY	TO FIND	SYMBOL
LENGTH				
mm	millimeters	0.039	inches	in
m	meters	3.28	feet	ft
m	meters	1.09	yards	yd
km	kilometers	0.621	miles	mi
AREA				
mm^2	square millimeters	0.0016	square inches	in^2
m^2	square meters	10.764	square feet	ft^2
m^2	square meters	1.195	square yards	yd^2
ha	hectares	2.47	acres	ac
km^2	square kilometers	0.386	square miles	mi^2
VOLUME				
mL	milliliters	0.034	fluid ounces	fl oz
L	liters	0.264	gallons	gal
m^3	cubic meters	35.314	cubic feet	ft^3
m^3	cubic meters	1.307	cubic yards	yd^3
MASS				
g	grams	0.035	ounces	oz
kg	kilograms	2.202	pounds	lb
Mg (or "t")	megagrams (or "metric	1.103	short tons (2000 lb)	T
TEMPERATURE (exact degrees)				
°C	Celsius	1.8C+32	Fahrenheit	°F
ILLUMINATION				
lx	lux	0.0929	foot-candles	fc
cd/m^2	candela/m^2	0.2919	foot-Lamberts	fl
FORCE and PRESSURE or STRESS				
kN	kilonewtons	0.225	1000 pound force	kip
N	newtons	0.225	pound force	lbf
kPa	kilopascals	0.145	pound force per square inch	lbf/in^2

*SI is the symbol for the International System of Units. Appropriate rounding should be made to comply with Section 4 of ASTM E380.

1. Report No.	2. Government Accession No.	3. Recipient's Catalog No.
4. Title and Subtitle End Region Detailing of Pretensioned Concrete Bridge Girders		**5. Report Date** March 2013
		6. Performing Organization Code
7. Author(s) B. E. Ross, G. R. Consolazio, and H. R. Hamilton		**8. Performing Organization Report No.**
9. Performing Organization Name and Address University of Florida Department of Civil & Coastal Engineering P.O. Box 116580 Gainesville, FL 32611-6580		**10. Work Unit No. (TRAIS)**
		11. Contract or Grant No. BDK75 977-05
12. Sponsoring Agency Name and Address Florida Department of Transportation Research Management Center 605 Suwannee Street, MS 30 Tallahassee, FL 32301-8064		**13. Type of Report and Period Covered** Final Report
		14. Sponsoring Agency Code
15. Supplementary Notes		

16. Abstract

End region detailing has significant effect on the serviceability, behavior, and capacity of pretensioned concrete girders. In this project, experimental and analytical research programs were conducted to evaluate and quantify the effects of different end region detailing schemes. Two end region design models were developed using results from the experimental and analytical programs. The first model can be used to design confinement reinforcement to prevent lateral-splitting failure at ultimate strength. The second model focuses on serviceability criteria and can be used to calculate bottom flange stresses due to prestressing and thereby assess the likelihood of bottom flange cracking in the end region.

The experimental program was conducted using (14) Florida I-Beam (FIB) specimens. Cracking and strain data were collected during prestress transfer and during the months following transfer. These data were used to evaluate serviceability criteria. Following serviceability evaluations, specimens were load tested to determine capacity and behavior due to applied loads. Specimens were loaded in three-point bending at a shear-span-to-depth (a/d) ratio of approximately 2.0. Variables considered in the experimental work included confinement reinforcement, steel bearing plates, horizontal reinforcement, vertical reinforcement, strand quantity, strand shielding, and strand layout.

The analytical program was conducted using finite element analysis (FEA). FEA models were validated using data from the experimental program. Variables considered in the analytical program included bearing pad geometry, bearing pad stiffness, steel bearing plates, transfer length, and prestress release sequence.

A test program was also conducted to evaluate the shear strength of 1950s era pretension girders used in the Florida highway system. These girders are of interest because they have thin 4 in. webs and very little specified shear reinforcement. Six test girders were removed from an existing bridge and were tested to failure in the laboratory. Results from the testing will be useful in determining the shear strength of similar pretensioned girders.

Recommendations are provided with regard to detailing of confinement reinforcement, embedded bearing plates, strand shielding, and crack control. Recommendations are also given regarding evaluation of early pretensioned girders.

G17. Key Word	18. Distribution Statement
Prestressed Concrete, End Region, Confinement Reinforcement, Splitting Failure, Shear, Debonding, Strand Shielding, Bridge Girders, Florida I-Beam	No restrictions. This document is available to the public through the National Technical Information Service, Springfield, VA, 22161

19. Security Classif. (of this report) Unclassified	20. Security Classif. (of this page) Unclassified	21. No. of Pages 581	22. Price

Form DOT F 1700.7 (8-72)   Reproduction of completed page authorized

Acknowledgments

Executive Summary

End region detailing has significant effect on the serviceability, behavior, and capacity of pretensioned concrete girders. In this project, experimental and analytical research programs were conducted to evaluate and quantify the effects of different end region detailing schemes. Two end region design models were developed using results from the experimental and analytical programs. The first model can be used to design confinement reinforcement to prevent lateral-splitting failure at ultimate strength. The second model focuses on serviceability criteria and can be used to calculate bottom flange stresses due to prestressing and thereby assess the likelihood of bottom flange cracking in the end region.

The experimental program was conducted using (14) Florida I-Beam (FIB) specimens. Both FIB-54 and FIB-63 specimens were used. Cracking and strain data were collected during prestress transfer and during the months following transfer. These data were used to evaluate serviceability criteria. Following serviceability evaluations, specimens were load tested to determine capacity and behavior due to applied loads. Specimens were loaded in three-point bending at a shear-span-to-depth (a/d) ratio of approximately 2.0. Variables considered in the experimental work included confinement reinforcement, steel bearing plates, horizontal reinforcement, vertical reinforcement, strand quantity, strand shielding, and strand layout.

The analytical program was conducted using finite element analysis (FEA). FEA models were validated using data from the experimental program. Variables considered in the analytical program included bearing pad geometry, bearing pad stiffness, steel bearing plates, transfer length, and prestress release sequence.

A test program was also conducted to evaluate the shear strength of 1950s era pretension girders used in the Florida highway system. These girders are of interest because they have thin 4 in. webs and very little specified shear reinforcement. Six test girders were removed from an existing bridge and were tested to failure in the laboratory. Results from the testing will be useful in determining the shear strength of similar pretensioned girders.

Recommendations are provided with regard to detailing of confinement reinforcement, embedded bearing plates, strand shielding, and crack control. Recommendations are also given regarding evaluation of existing 1950's era pretensioned girders.

Table of Contents

List of Figures

List of Tables

1   Introduction

In January 2009, the Florida Department of Transportation (FDOT) mandated that all new prestressed concrete bridges in Florida be constructed using the new Florida I-Beam (FIB) sections. The standard FIB end region reinforcement is based on historic FDOT details, American Association of State Highway and Transportation Officials (AASHTO) Load and Resistance Factor Design (LRFD) Bridge Design Specifications (LRFD 2010), and constructability considerations. End region detailing has a significant effect on the strength and behavior of pretensioned I-girders. Effective detailing enables the end region to serve two critical functions. First, the end region transfers prestressing forces from the strands to the cross-section. Second, the end region transfers shear force from the girder into the bearing. A limitation in the current AASHTO LRFD is the use of empirical design provisions for portions of the end region reinforcement with no consideration of the flange geometry, prestressing force, or strand pattern.

This report presents the results of experimental and analytical investigations that were conducted to evaluate the effects of end region detailing on strength and serviceability of bridge girders. Also included in the report are proposed models that can be used to design effective end region details.

Experimental work in this project included load tests of 32 pretensioned, precast girder specimens. Specimens were loaded in three-point bending and ranged in size from 28 in. to 63 in. deep. Load tests were conducted as part of four different test programs: Small beam, SR-72, FIB-54, and FIB-63. The SR-72 test program utilized girders salvaged from a bridge demolition, whereas the other three test programs utilized girders constructed specifically for experimental testing.

Analytical work in this project utilized the finite element (FE) analysis method. FE models were linear-elastic and were intended to model the behavior of the end region prior to cracking. FE models were validated using data from the experimental program and were then used to examine parameters that were not investigated experimentally such as bearing pad width, bottom flange geometry, and strand debonding patterns. The effects of applied loads and prestressing forces were considered in the FE analyses.

Building on the experimental and FE results, two analytical models were developed to aid in the design of effective end region details. The first is an ultimate strength model to design confinement reinforcement. The second is for calculating lateral stresses in the bottom flange due to prestressing.

1.1 Objectives

Combined experimental and analytical work was conducted to achieve the following objectives:

- Evaluate strategies for controlling or preventing web splitting cracks including vertical post-tensioning; strand shielding beyond AASHTO LRFD allowances; and strategic use of vertical reinforcement.

- Determine the function(s) of confinement reinforcement during prestress transfer and at ultimate strength.

- Create a model for bottom flange splitting cracks at prestress transfer.

- Create a design model for confinement reinforcement at ultimate strength.

- Evaluate the effects of strand shielding beyond AASHTO LRFD allowances on the ultimate strength and serviceability of FIB girders.

- Evaluate the need (or lack thereof) for confinement reinforcement within the transfer length of partially shielded strands.

- Evaluate the contribution of horizontal vertical reinforcement in end region.

- Develop recommendations regarding end region detailing practices.

- Evaluate the shear strength and behavior of early pretensioned girders used in Florida highway bridges.

1.2 Report Outline

The report is divided into a summary document and several appendixes. This portion of the report is the summary document, which is comprised of nine chapters. Table 1 shows the correspondence between the chapters in this summary document and the appendixes, which present the research in greater detail than the summary document.

Table 1–Report organization

Topic	Summary Chapter	Appendix
Introduction	1	--
Background	2	--
Literature Review	--	A
Small Beam Test Program	3	B
SR-72 Test Program	4	C
FIB-54 Test Program	5	D
FIB-63 Test Program	6	E
Analytical Program (Finite Element Analyses)	7	F
End Region Design Models	8	G
Recommendations	9	--
Support Data	--	H

2   Background

The state of Florida has over 12,000 bridges in its public road system (FHWA 2010). Prestressed concrete is the most utilized material in Florida bridges, with precast-pretensioned concrete I-girders being the most common structural element. Figure 1 shows a typical highway overpass in Florida. It consists of multiple simple spans with each simple span being comprised of multiple individual I-girders.

Figure 1–Prestressed concrete bridge

Because Florida relies heavily on concrete I-girders there is motivation to improve the efficiency and performance of these members. To that end the Florida Department of Transportation (FDOT) introduced the Florida I-Beam (FIB) in 2009 for use in new bridge construction and bridge widening projects. The FIB was designed to be "more efficient to fabricate, safer to construct, and more cost effective" than the formerly used AASHTO and Florida Bulb-T shapes (FDOT 2009). FIB sections range from 36-in. deep to 96-in. deep and have the same top and bottom flange geometry regardless of depth (Figure 2). Because the bottom flange is relatively wide, it can accommodate up to 72 prestressing strands, thus improving the structural efficiency of the sections, particularly for those constructed with concrete strengths greater than 8000 psi.
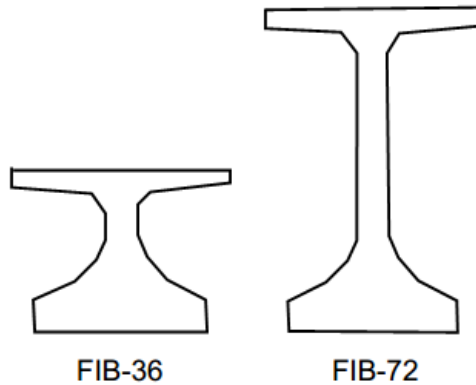
Figure 2–Florida I-Beam cross-sections

Although beneficial with regard to structural efficiency, the relatively wide bottom flange and high prestress forces in FIB girders raise potential concerns for capacity and serviceability. One failure mode accentuated by a wide and narrow flange is lateral-splitting, which occurs when the bottom flange splits laterally above the bearing due to applied loads (Figure 3). This behavior has been observed in experimental testing (Llanos et al. 2009) and in beams with slender bottom flange geometry. If the end region is not appropriately detailed lateral-splitting failure can control the shear capacity of I-girders and can lead to situations where the code calculated shear capacities are unconservative. Investigation of lateral-splitting failure was a primary focus of the experimental and analytical studies presented in this report.
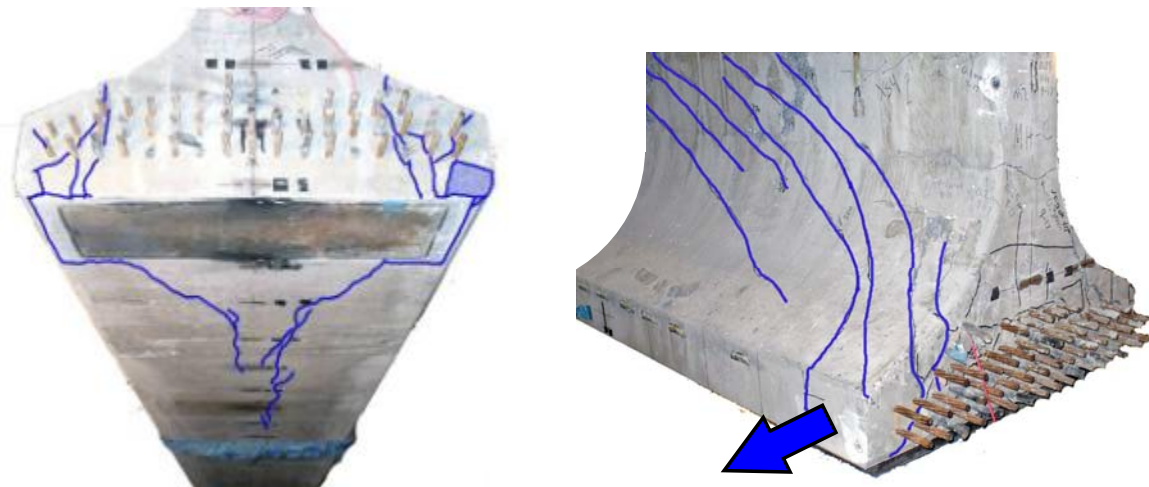
Figure 3–Lateral-splitting failure

Another focus of the research was controlling - and if possible preventing - end region splitting cracks. Web splitting cracks are an ongoing issue in I-girders. These cracks occur due

to vertical tensile stresses that form as prestressing is spread from the bottom flange to the entire cross-section. Splitting cracks in the bottom flange have historically been less common than those in the web. Recently, however, flange splitting cracks have been observed in girders with slender bottom flanges (Figure 4). Because FIB girders have relatively slender bottom flanges there is motivation to investigate flange splitting cracks, as well as, splitting cracks in the web.

Figure 4–Flange splitting crack (Tadros et al. 2010)

This report also presents experimental results of testing on early (circa 1950s) pretensioned girders utilized in Florida. Early girder designs in Florida called for thin 4 in. webs and very little shear reinforcement. Accordingly these girders also have low code-calculated shear capacity, which presents a problem with load rating. To more accurately determine shear capacity, load tests were conducted using specimens salvaged from a demolished bridge. The effect of integral curbs and barriers on shear capacity and behavior was also investigated during load testing. Results of these tests may be useful in load rating the shear capacity of similar girders still in service.

3   Small Beam Tests

The AASHTO LRFD Bridge Design Specifications require that confinement reinforcement be placed around prestressing strands in the bottom bulb of pretensioned concrete beams. Although the AASHTO specifications contain prescriptive requirements for the quantity and placement of confinement reinforcement, the effect of such reinforcement on the end region behavior is not well understood. To evaluate the function and effect of confinement reinforcement, twelve tests were conducted on 28-in. deep precast-pretensioned beams. Beams were loaded in three-point bending at a shear span-to-depth ratio of 1.0. Variables in the test program included strand size, strand quantity, prestressing force, and the presence or lack of confinement reinforcement. See Appendix B for a comprehensive discussion of testing and results.

3.1   Specimen Details and Test Setup

Six precast pretensioned concrete beams from a previous research project (O'Neill and Hamilton 2009) were salvaged for use in testing the end region. That research project conducted tests to measure service stresses at mid-span without loading the beams to their ultimate strength. The ends remained undamaged and were fit for the shear tests reported in this chapter. Strand diameter, strand quantity, prestress force, and confinement reinforcement were included in the variables examined (Figure 5).

The beams were constructed so that each end had identical confinement reinforcement. To create specimens with no confinement reinforcement, one end of each beam was saw-cut to remove the portion containing the confinement steel (Figure 6). Each end of each beam was then tested in three-point bending (Figure 7). Tests on specimens (ends) with confinement reinforcement are referred to as "confined tests" and those on specimens without confinement reinforcement as "unconfined tests".

Load, strain, displacement and strand slip data were collected during testing.
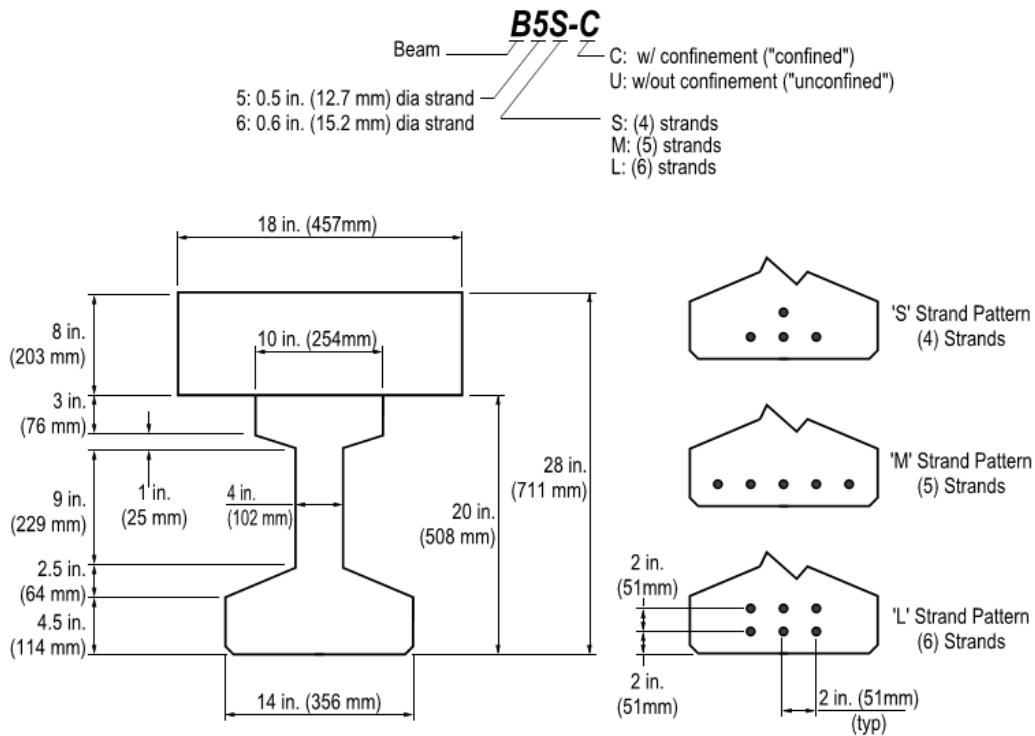
Figure 5–Nomenclature and beam details
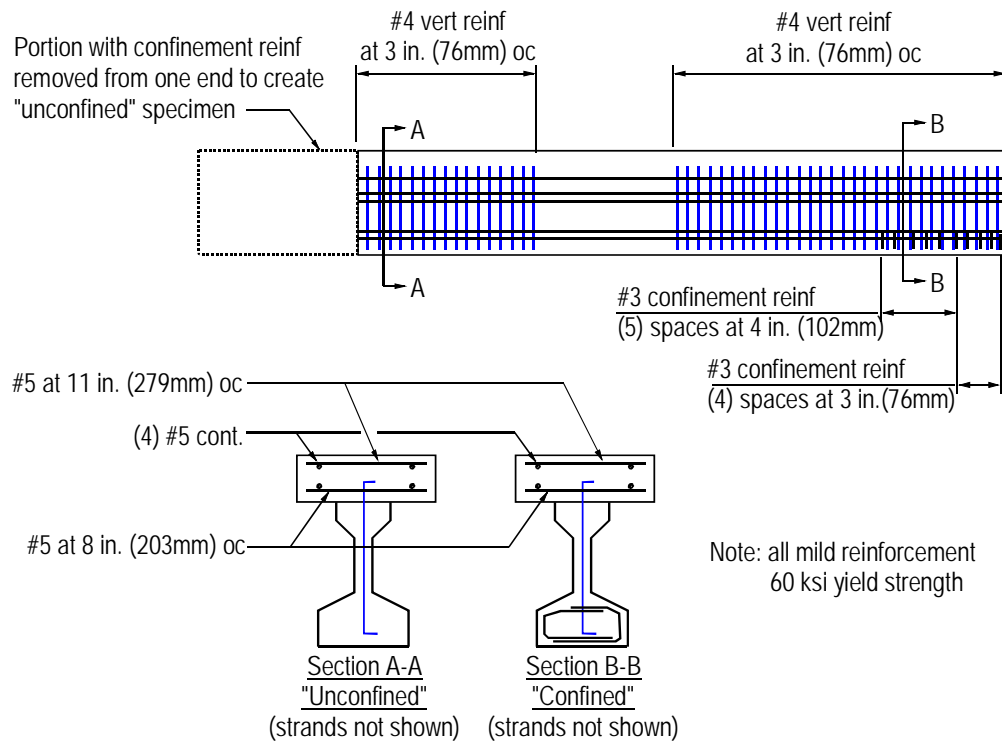
Figure 6–Reinforcement details
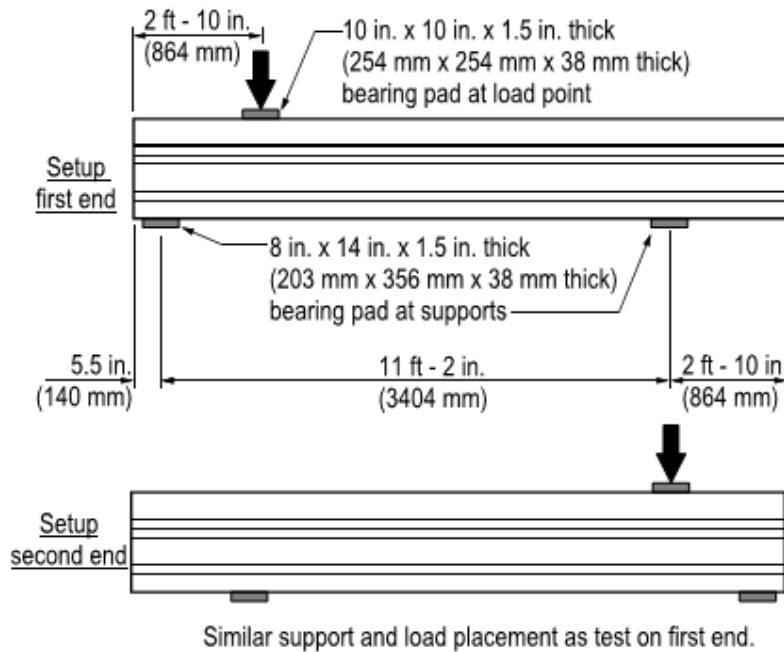
Figure 7–Test setup

3.2 Results and Discussion

To illustrate the general differences in behavior between confined and unconfined specimens, Figure 8 shows the load-displacement and strand-slip results for confined (B5M-C) and unconfined (B5M-U) specimens. The figure shows vertical displacement at the load point and average slip of bonded strands. Since the two tests were conducted on the same beam, the strand pattern, strand size, prestress force, and concrete were identical for both tests, with the confinement reinforcement being the only difference. The qualitative behavior of these specimens is representative of all six pairings of similar confined and unconfined tests.

Both specimens behaved in a linear-elastic manner until reaching a load of approximately 100 kip (445 kN). Initial cracks consistently formed in the web and were inclined between the load point and the support, whether or not the specimen contained confinement reinforcement. Flexural cracks and additional inclined cracks formed as the load was further increased. When the load reached 150kip (668 kN), the inclined cracks in both tests had propagated into the bottom bulb, thereby reducing the available development length of the prestressing strands, and

initiating strand slip. Strand slip was gradual at first, but increased when the load reached approximately 175 kip (779 kN). Slip and displacement characteristics of the confined and unconfined ends remained similar up to a load of 190 kip (846 kN), at which point the unconfined specimen failed in a splitting mode. Splitting failures were characterized by formation of splitting cracks at the end of the beam above the support, accompanied by sudden strand slip and an almost instantaneous loss of capacity.
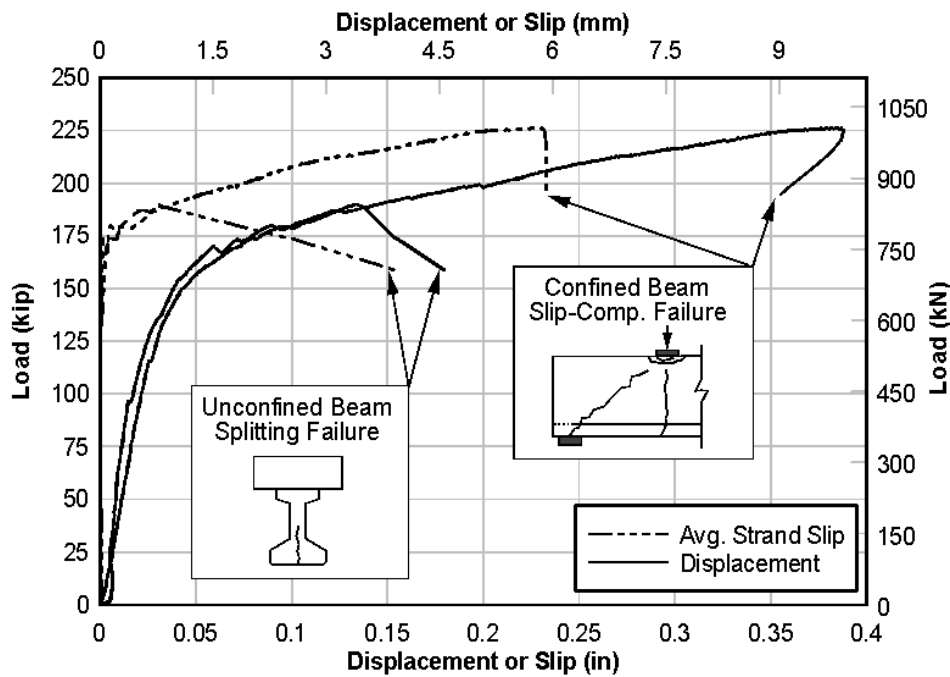
Figure 8–Load vs. displacement and strand slip

For the confined end, load continued to increase until failure occurred at a load of 226 kip (1006 kN). The continued load increase, however, was accompanied by further strand slip indicating that the remaining development length provided sufficient anchorage to maintain stability of the mechanism. As the strands slipped, the diagonal crack opened further, reducing the concrete area available to resist the compression in the top of the section. Capacity was reached when the concrete below the load point was crushed due to the excessive rotation that was allowed, in part, by strand slip. Indeed most of the rotation occurred about the inclined crack, which shortened the available strand development length. Strands in the confined end slipped 0.23 in. (5.8 mm) at failure. Enhanced photographs of the failed test specimens are shown in Figure 9.

Splitting failure in
unconfined specimen
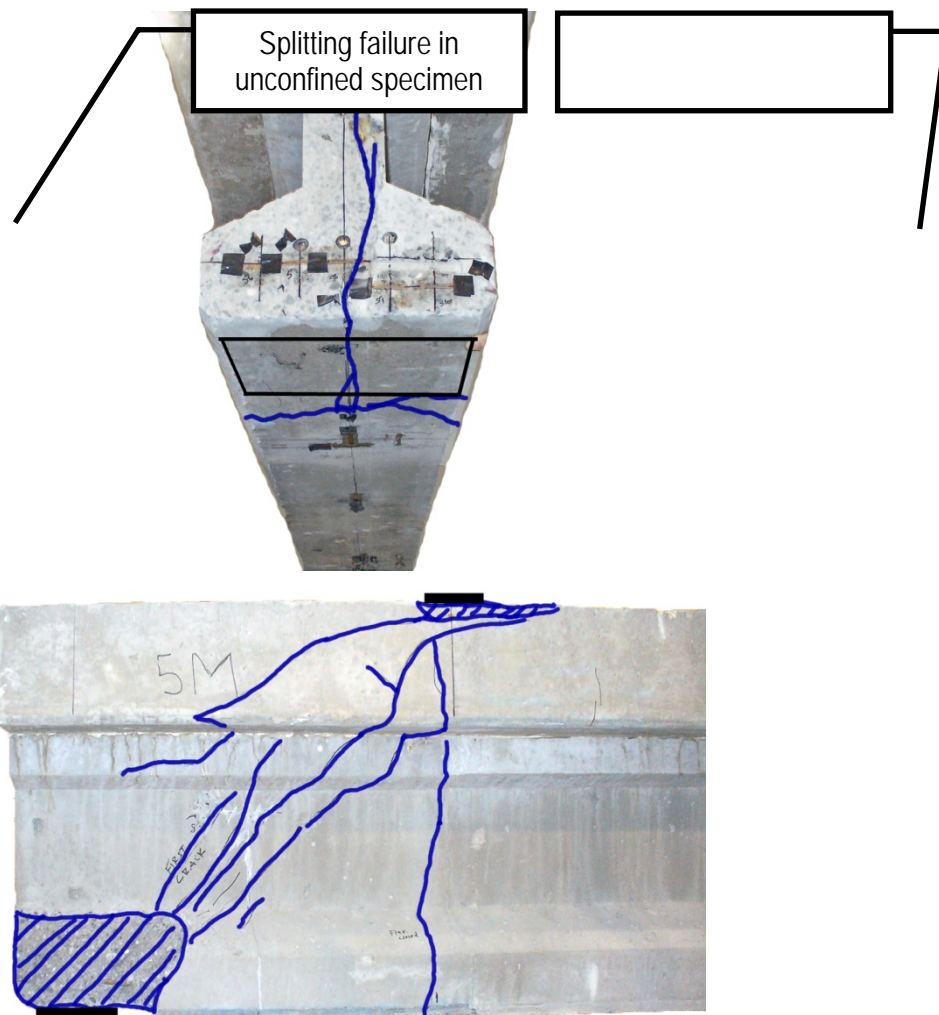
Figure 9–Failure of unconfined (left) and confined (right) specimens

In addition to the typical behavior described above, some common behavioral characteristics were noted in all tests. Strand slip occurred in all specimens after cracks had propagated into the bottom bulb. Furthermore, the load at which this slip occurred was at or near the same load for each pair of confined and unconfined tests conducted on a single beam. Thus confinement reinforcement did not prevent or delay strand slip, but did allow strands in the confined beams to continue carrying tensile forces even as they slipped beyond the point at which the unconfined tests failed in splitting. Slip at maximum load was, on average, over seven times greater in the confined tests than in the unconfined tests. While significant strand slip occurred in the confined beam tests upon reaching peak load, section curvature was not always sufficient at this point to crush the compression zone, thus causing a definitive drop in load and

signal the end of the test. In such cases, an arbitrary amount of additional displacement was imposed to ensure that the ultimate load had indeed been reached.

Figure 10 shows the normalized shear capacity for each test. The experimental shear capacity is defined as the shear force at the near support corresponding to the maximum load. Values have been normalized by the average of the unconfined beam capacities: 138 kip (614 kN). The data clearly indicate that variation in strand diameter had little effect on the shear capacity in unconfined tests. Average capacity of the unconfined tests with 0.5-in. (12.7 mm) diameter strand (B5 in the figure) and 0.6-in. (15.2 mm) diameter strand (B6 in the figure) varied by only 4%, indicating that strand size and area of prestressing steel did not significantly affect the capacity of the unconfined beams.

Confined tests resulted in an average of 25% more shear capacity than that of the unconfined tests and more than twice the displacement ductility. The improved shear capacity was likely due to increased contribution from the mild reinforcement. As the confined beams rotated beyond the point at which the unconfined beams split and failed, forces in the vertical steel increased, leading to improvements in shear capacity. The increased rotation also caused the resultant of the compressive force to move upwards, thereby increasing the moment arm and shear contribution of the prestressing strands. The experimental shear capacities were an average of 34% greater than the shear capacities calculated by the general procedure in section 5.8.3.4.2 of AASHTO LRFD (2007).
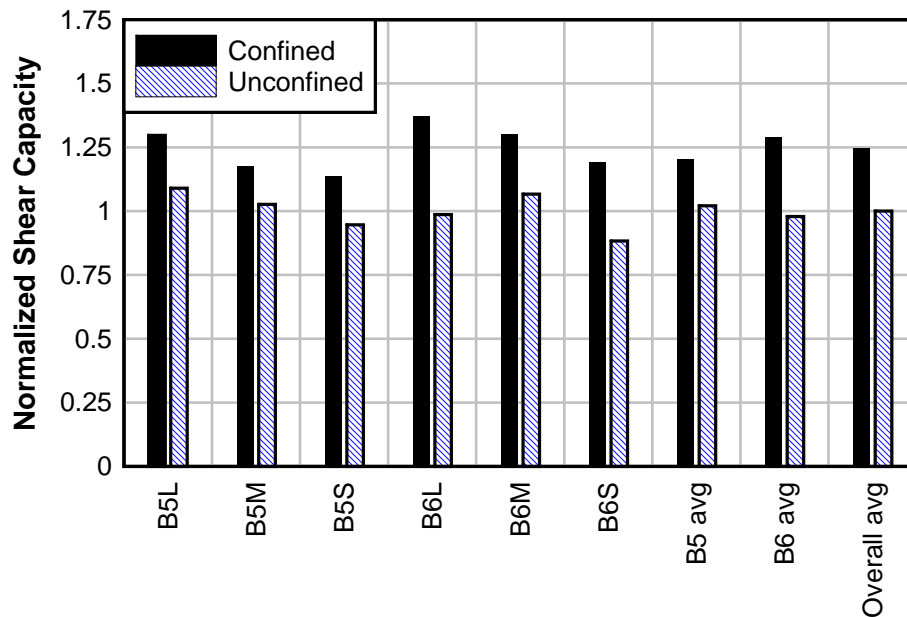
Figure 10–Normalized shear capacity

3.3   Conclusions

Twelve precast-prestressed test specimens were loaded to failure in three-point bending. The load point was placed approximately one member depth away from the support. Half of the specimens had confinement reinforcement and the other half did not. Other variables in the test program included the quantity and size of prestressing strands. Conclusions are listed below. See Appendix B for additional discussion and justification of the conclusions.

- Confinement reinforcement had negligible effect on measured strain distribution in concrete prior to cracking.
- Transverse tensile strains formed in the bottom flange above the bearing pad. The maximum strain occurred at the centerline of the cross-section and the strain diminished to a minimum at the edge of the flange. Transverse tensile strains are believed to have led to splitting failures in the beams without confinement reinforcement.
- Confinement reinforcement did not consistently delay or prevent slipping of prestressing strands. Such reinforcement, however, did provide sufficient slip restraint

to the strands to ensure that they were able to continue supporting tensile forces beyond the point at which the unconfined test specimens failed.

- Confinement reinforcement prevented splitting failure, thereby improving the shear capacity and displacement ductility of the confined tests relative to the unconfined tests. Average shear capacity increase was 25% and the average increase in displacement ductility was 157%.

- Experimental results and strut-and-tie modeling suggest that the strands were 30% developed on average at peak load. Development of the strands in the experimental tests was limited by the formation of cracks within the strand development length.

4   SR-72 Tests

Ultimate load tests were conducted on precast pretensioned girders that were removed from a Florida bridge after nearly 55 years of service. The shear capacity of these girders is of interest because they had relatively thin webs and limited vertical reinforcement. Varying portions of the deck and/or curb were retained with each girder to evaluate the effect of these elements on shear capacity. Girders were loaded in three-point bending at shear-span-to-depth (a/d) ratios ranging from 2.1 to 4.5. Results of this testing will be helpful in evaluating the strength of similar girders that are still in service. A summary of the SR-72 test program is presented in this chapter. See Appendix C for a more comprehensive discussion of testing and results.

4.1   Specimen Details and Test Setup

Test girders were salvaged from a bridge on Highway SR-72, in Sarasota County, Florida. Girders were precast and pretensioned, having the cross-section shown in Figure 11. Varying widths of the composite concrete bridge deck were kept integral with each salvaged girder. Portions of the integral curb were also retained with the two exterior girders used in the test program. Specified reinforcement in the girders and deck is shown in Figure 12 and Figure 13. Destructive and non-destructive investigation indicated transverse reinforcement in the girders was less than specified on the original drawings. Girder labels and cross-sections are shown in Figure 14.

Girders were tested in three-point bending. Dimensions and setup are described in Figure 15 and Table 2. Load, displacement, strain, and strand slip data were collected during testing. As indicated in the table, SR-72 specimens were load tested at one end rather than each end as was done for other specimens in this research project.
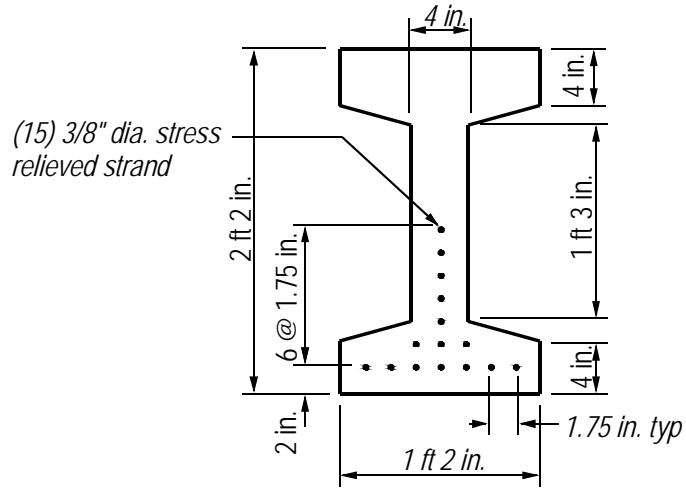
Figure 11–SR-72 cross-section and prestressing
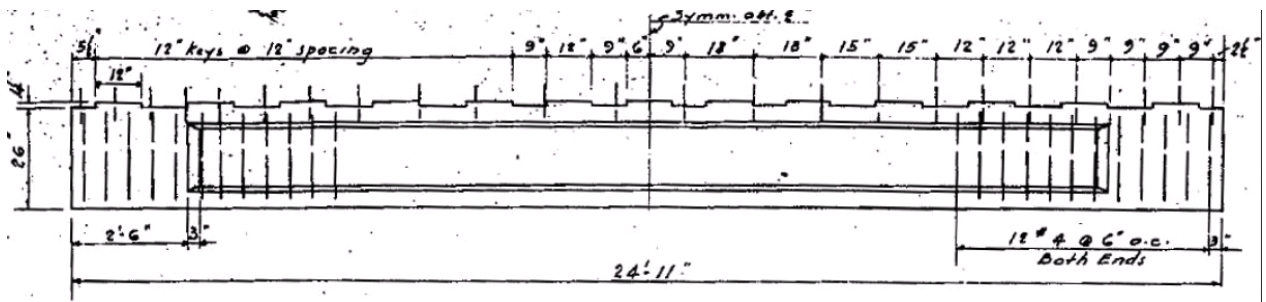
Figure 12–Specified transverse reinforcement
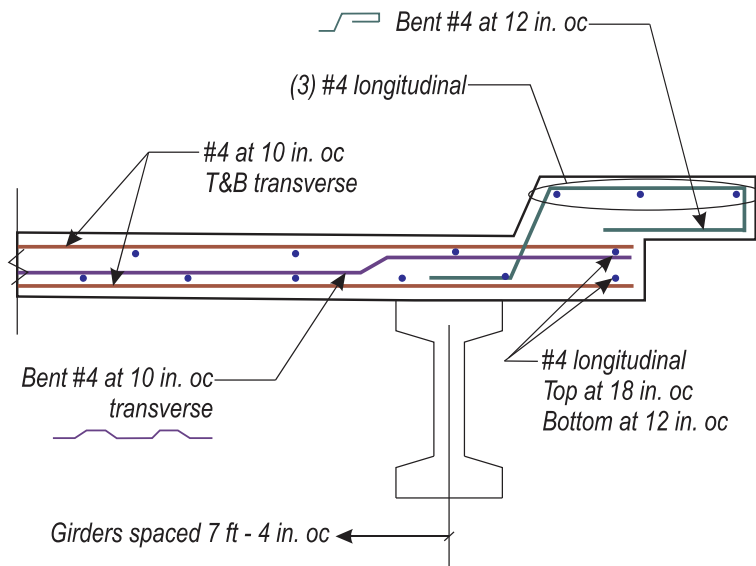
Figure 13–Specified deck and curb reinforcement
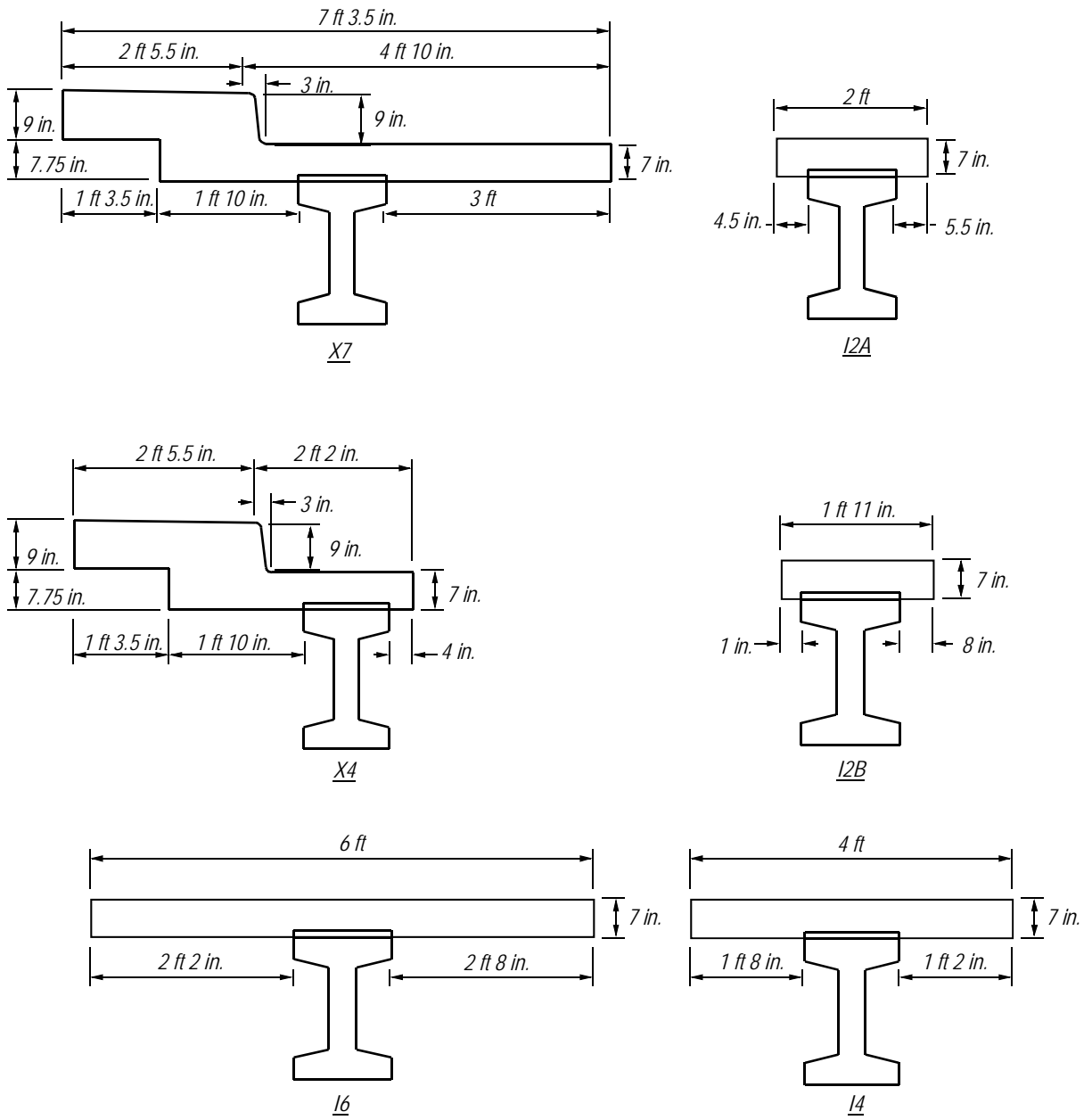
Figure 14–SR-72 specimens and labels
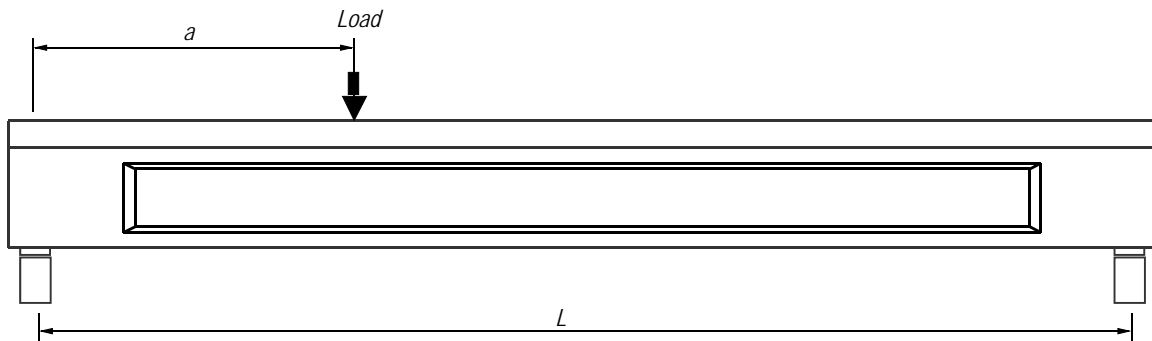
Figure 15–Test setup

Table 2–Test setup dimensions

Girder	A	a/d*	L
X7	8'-2"	3.4	23'-9"
X4	8'-2"	3.4	24'-3"
I2A	10'-11"	4.5	23'-9"
I2B	8'-1"	3.3	24'-11"
I4	5'-2"	2.1	23'-10"
I6	8'-2"	3.4	24'-0"
*d = 29 in.			

4.2 Results and Discussion

As load was applied, behavior was linear- elastic until the formation of a crack, which was typically a flexural crack located below the load point (Figure 16). As the load increased, inclined cracks formed in the web. Additional inclined cracks formed at flatter angles and closer to the supports as testing continued. During the latter stages of loading but before ultimate strength was reached, the inclined cracks were wide enough to allow the passage of light. Peak load was controlled by capacity of the compression zone in girders X7, X4 and I2A, and by formation of inclined cracks in girders I2B, I4 and I6.

Figure 16 shows the crack pattern for specimen I2B. Similar crack patterns were observed in the other girders. Figure 16 also shows the location of vertical reinforcement as determined by non-destructive testing for this specimen. The location and quantity of vertical reinforcement was different from the reinforcement specified in the construction drawings. Inclined cracks in the specimens typically did not intersect vertical reinforcement.
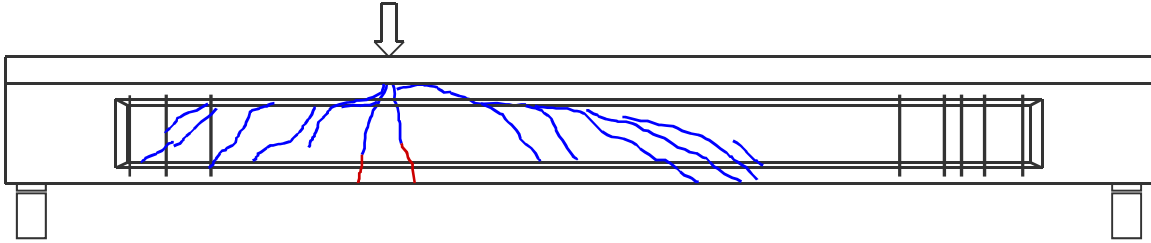
Figure 16–Crack pattern girder I2B (initial crack shown in red)

Because the inclined cracks were relatively wide as the specimen was near ultimate strength, and because the inclined cracks did not typically intersect vertical reinforcement, a plastic truss could not form. Rather, the girders behaved as tied-arches with shear forces being transferred through compression in the concrete arch. Tied-arch behavior was typical for all girders. Truss and tied-arch action are discussed and defined in the literature review contained in Appendix A.

As previously noted, peak load of girders X7, X4 and I2A was controlled by capacity of the compression zone. Peak load for girders I2B, I4 and I6 corresponded to formation of inclined cracks in the web. Table 3 summarizes the behavior at peak load of each girder.

Table 3–SR-72 girder behaviors at peak load

Girder	Behavior at Peak Load
X7	Punching failure of concrete arch below the load point.
X4	Flexure compression failure of concrete near the load point.
I2A	Instability (buckling) of concrete compressive arch.
I2B	Formation of inclined crack in web.
I4	Formation of inclined crack in web.
I6	Formation of inclined crack in web.

Figure 17 compares the experimental capacities with the code-calculated nominal shear capacities. Calculations were based on the specified properties of an interior girder and are plotted in Figure 17 as a function of the shear span a. The abrupt change in capacity at $a = 5.8$ ft corresponds to the specified end of vertical reinforcement. Girders performed well in the load tests in spite of thin webs, minimal shear reinforcement, and 55 years of service. In each case, the experimental shear capacity was greater than the code-calculated capacity.
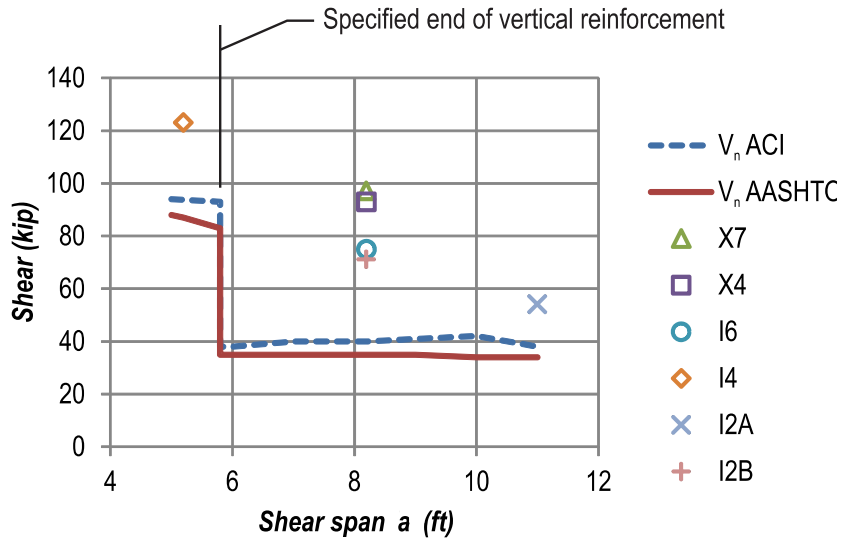
Figure 17–Experimental and code shear capacities

4.3   Conclusions

Six pretensioned concrete girders were salvaged from an existing bridge and tested after nearly 55 years of service. Girders were tested in three-point bending at a/d ratios from 2.1 to 4.5. Varying portions of the existing deck and/or curb were retained with each test girder. The experimental results were compared to theoretical predictions of strength capacity. Key conclusions are listed below. Additional conclusions, as well as discussion and justification of conclusions are presented in Appendix C.

- Test girders behaved as tied arches during the latter stages of loading. This is evident from the relatively wide cracks that did not allow aggregate interlock and from the absence of transverse reinforcement necessary to ensure plastic truss behavior.
- Tied-arch behavior controlled the experimental strength of girders X7, X4 and I2A. Arches in these girders failed due to punching, flexural compression, and arch instability, respectively.
- For girders I2B, I4, and I6 the maximum load occurred just prior to the formation of an inclined crack in the web. These girders behaved as tied-arches during the latter stages of loading, however, their maximum capacities were limited by the capacity of the web to resist inclined cracking.

- For tests at the same a/d ratio, the cast-in-place curb increased the average exterior girder strength by 30% over that of the interior girders with no curb.

- Nominal shear capacities calculated by ACI 318 and AASHTO LRFD methods were conservative relative to the experimental results. On average, the ratio of experimental-to-calculated shear capacity was 2.0 for ACI 318 and 2.1 for AASHTO LRFD calculations.

- The experimentally determined prestress force in specimen I2A was 47% less than the specified prestress. The large difference between the specified and experimental values may indicate quality control issues in addition to higher than expected losses.

- In spite of relatively thin webs, small quantities of vertical reinforcement, and poor quality control during construction, the girders were able to support significant shear force after nearly 55 years of service.

5   FIB-54 Tests

Five 54-in. deep Florida I-Beam (FIB-54) girders were fabricated and load tested to evaluate the effects of different end region details on girder capacity and behavior. Each end of each girder was detailed differently, which resulted in ten unique test specimens. Variables in the end region detailing included: presence or absence of embedded steel bearing plates, quantity and configuration of confinement reinforcement, strand bond pattern, strand quantity, and quantity of horizontal and vertical end region reinforcement.

Strain and crack data were collected during and after prestress transfer to evaluate the effectiveness of each detailing scheme on controlling bottom flange cracking. Load tests were then conducted on each specimen (end) to determine the effects of each detailing scheme had on girder behavior and capacity. Specimens were loaded in three-point bending at a shear span-to-depth ratio of 2.0. Failure modes included web-shear, bond-shear, and lateral-splitting.

5.1   Specimen Details and Test Setup

Five 50-ft. long FIB-54 girders were built according to the schedule of variables shown in Table 4. Each end of each girder was detailed differently, resulting in ten unique specimens. Girder and specimens were labeled using the convention shown in Figure 18. Girders were built in two different phases. Phase 1 girders were built by Dura-Stress of Leesburg, FL. Phase 2 girders were built by Standard Concrete Products of Tampa, FL. Construction plans, materials properties, and construction timelines are presented in detail in Appendix D. Figure 20 shows specimens HC and VU. These specimens had the most (HC) and least (VU) amounts of end region mild reinforcement.

Strain, crack, and material property data were collected during fabrication. Vibrating wire and electrical resistance strain gages were used to collect strain data. Crack data were collected using a tape measure and microscope. Material property data were collected for concrete compressive strength, reinforcement yield strength and elongation, prestressing strand strength, and prestressing strand bond capacity. The Standard Test for Strand Bond (NASP 2009) was used for determining strand bond capacity.

Table 4–FIB-54 test girder and specimen variables

Test Girder	Specimen	Bearing plate	Mild reinforcement		Strand bond pattern	Confinement reinforcement	Phase
			Vertical	Horizontal			
H	HC	Yes	FDOT	Yes	Design	FDOT	1
	HU	Yes	FDOT	Yes	Design	No	1
V	VC	Yes	Mod	No	Design	FDOT	1
	VU	Yes	Mod	No	Design	No	1
W	WN	No	FDOT	No	Web	Mod	2
	WB	Yes	FDOT	No	Web	Mod	2
F	FN	No	FDOT	No	Flange	Mod	2
	FB	Yes	FDOT	No	Flange	Mod	2
D	DC	Yes	FDOT	No	Design	FDOT	2
	DM	Yes	FDOT	No	Design	Mod	2
FDOT: Detailed per FDOT design standards							
Mod: Detailed with modifications to FDOT design standards							
Web: Fully bonded strands placed below web (24 fully bonded strands)							
Flange: Fully bonded strands placed in outer portion of flange (24 fully bonded strands)							
Design: Strand pattern based on prototype design (45 fully bonded strands)							

End designation
C: Confinement reinforcement per FDOT
U: No confinement reinforcement
B: Bearing plate included
N: No bearing plate
M: Modified confinement reinforcment

HC̄

Specimen label

Girder label
H: Horizontal reinforcement in end region
V: Modified vertical reinforcement in end region
W: Strands fully bonded below web
F: Strands fully bonded in outer flange
D: Strands bonded per design girder

Figure 18–FIB-54 labeling scheme
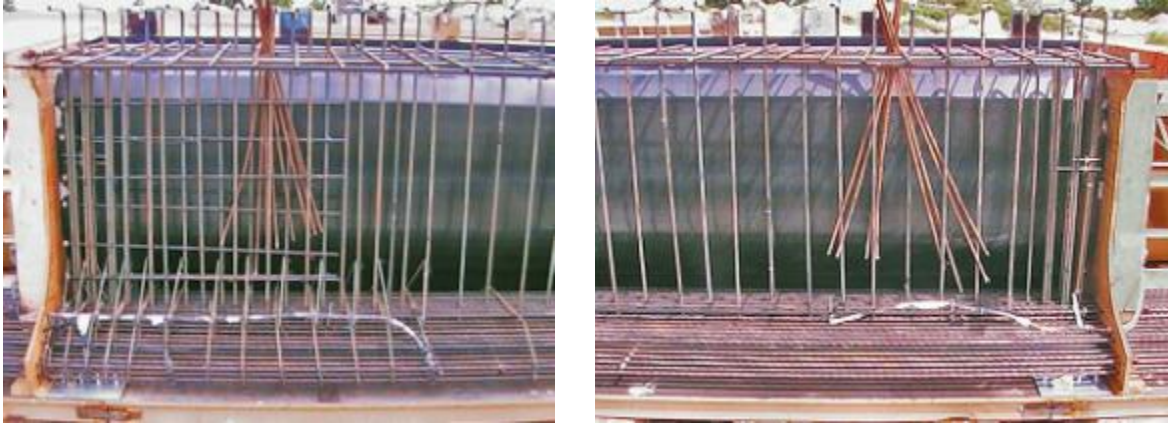
Figure 19–FIB-54 end region reinforcement for HC (left) and VU (right)

After fabrication, girders were trucked to the FDOT M.H. Ansley Structures Research Center in Tallahassee, FL. At the research center cast-in-place composite decks were built on top of each girder. Once the decks were sufficiently cured load tests were conducted. Each end (specimen) was loaded in 3-point bending as shown in Figure 20. After the first end was tested, the load point and supports were moved and the opposite end was tested. Photos of the test setup are shown in Figure 21. Load, displacement, strain, and strand-slip data were collected during load testing.
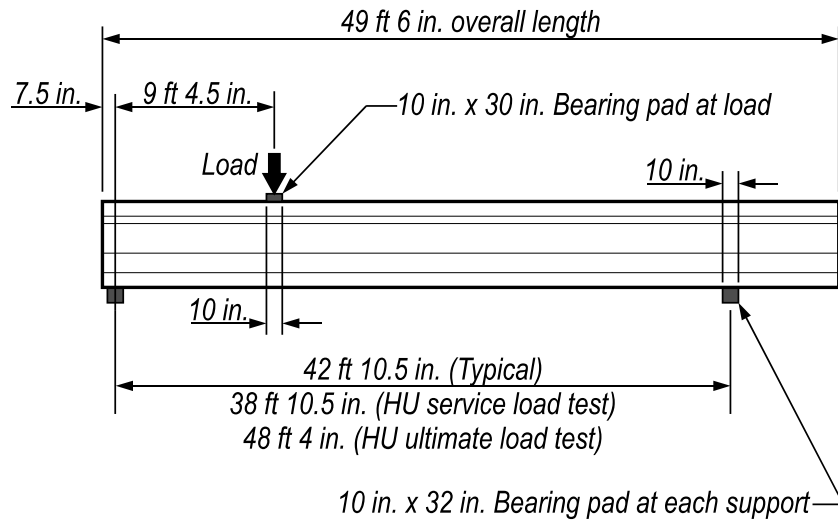
Figure 20–FIB-54 test setup
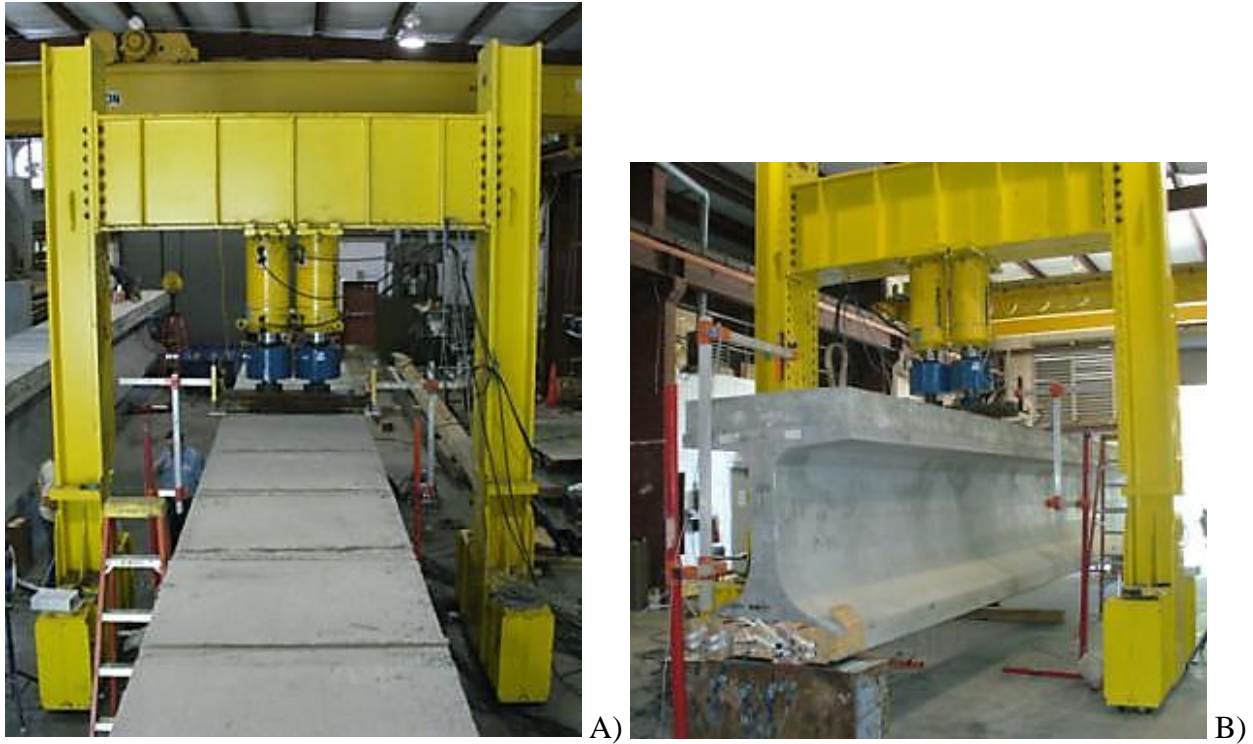
Figure 21–Test specimen and load frame view of A) top and B) side of girder

5.2   Results and Discussion

5.2.1   Strain during Prestress Transfer

Prestressing transfer in Florida is typically accomplished by flame cutting the prestressing strands, beginning with those on the outside of the strand pattern. Strands are cut sequentially starting with the outside strands and working toward the center of the beam. Strain gages labeled 'XS3' were placed at the end of specimens HC, HU, VC, and VU to monitor strain in the bottom flange during the prestress transfer (Figure 22).
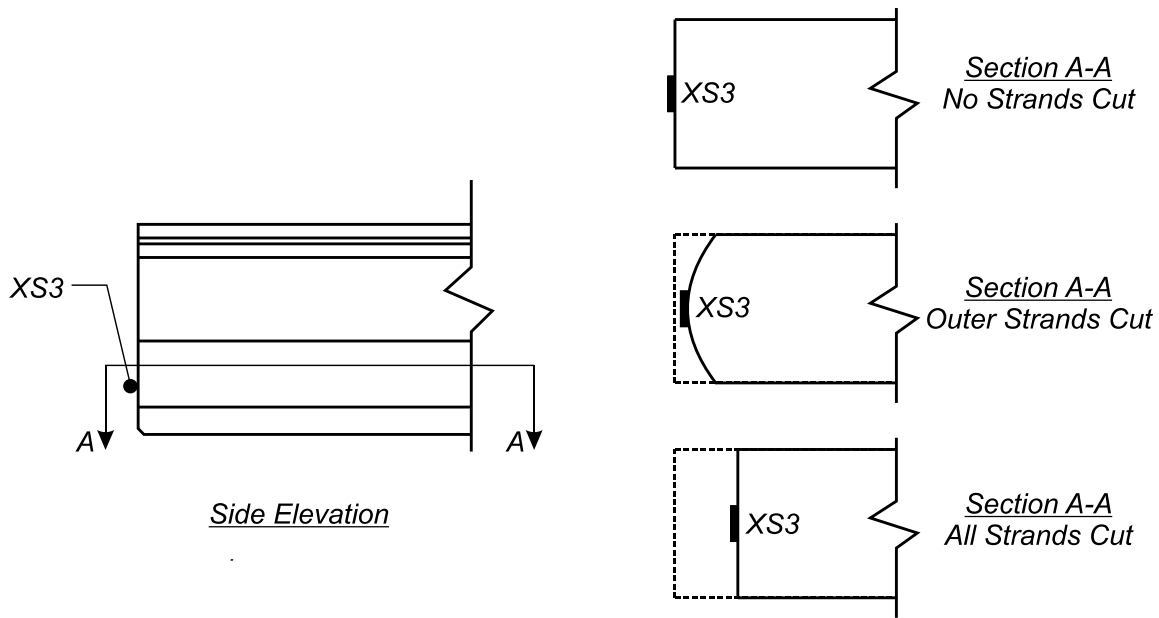
Figure 22–Flange displaced shapes

Data from gages XS3 are summarized in Table 5. The maximum tensile strain reported by XS3 occurred when only those strands in the outer portion of the flange were cut. The tensile strain reported by gages XS3 decreased significantly after the inner strands had been cut. This strain behavior is explained by the deformed shapes shown in Figure 22. Forces from the outer strand deform the edges of the flange resulting in transverse tension. Forces from the inner strands lead to a more uniform displacement across the bottom flange resulting in a reduction of transverse tension.

Table 5–Tensile strain during prestress transfer girders H and V

	Strain in specimens with confinement reinforcement (microstrain)		Strain in specimens without confinement reinforcement (microstrain)	
Gage and condition	HC	VC	HU	VU
X3 maximum tensile strain –outer strands cut	406	177	724	1258
X3 all strands cut (all strands released)	25	15	60	45

Assuming a concrete rupture strength of $7.5\sqrt{f'_c}$ and elastic modulus of $57{,}000\sqrt{f'_c}$, the expected rupture strain was approximately 135 microstrain. The maximum strain values reported by gages XS3 were larger than 135 microstrain - in some cases much larger - suggesting that cracks may have formed near the gage locations during the strand cutting process. Cracks were not visually observed, however, and it is believed that these cracks closed as the inner strands were cut.

Strain data presented above demonstrate that transverse tension forms in the bottom flange of I-girders due to prestress forces from the outer strands. This transverse tension is partially relieved as inner strands are cut.

5.2.2 Cracks due to Prestress

Crack data were also collected during and in the weeks following prestress transfer. Three types of cracks were observed:

- Top flange flexural cracks
- Web splitting cracks
- Flange splitting cracks

Top flange cracks formed due to flexural stresses generated by the vertically eccentric prestressing. Top flange cracks are outside the scope of the FIB-54 test program. Web splitting (Figure 23) cracks also formed due to eccentric prestressing. As the prestress force was distributed from the bottom flange to the rest of the cross-section, the attendant vertical tension stresses caused cracks in the web. Flange splitting cracks were of primary interest in the FIB-54 test program. Flange splitting cracks were caused by horizontal eccentricity of prestressing, Hoyer expansion of strands, and self-weight reaction of the girders.

Figure 23–Web splitting (blue) and flange splitting (brown) cracks

Web and flange splitting cracks were first observed nine days after prestress transfer for girders H and V, which were built during the first phase of construction. Girders W, F, and D were built in the second construction phase. Cracks in Girders W, F, and D were first observed during prestress transfer. For all girders, cracks typically grew in length and in quantity after they were first observed. Figure 24 shows the web and flange cracks in girders W, F, and D three months after prestress transfer. Length and area of the bottom flange cracks for these girders are quantified in Figure 25.

Each of the specimens listed in Figure 25 had the same Class of concrete, were fabricated at the same time, and were fabricated using the same procedures. Strand patterns, bearing plates, and confinement reinforcement varied among specimens. The most severe cracking, in terms of total length and area, occurred in specimens FB and FN. Severity of cracking in these specimens is attributed to the strand pattern. All of the fully bonded prestressing strands in these specimens were located in the outer portion of the flange. As discussed in the previous section, prestressing located in the outer portions of the flange caused transverse tension in the bottom flange. This transverse tension is culpable in the cracks observed in specimens FB and FN.
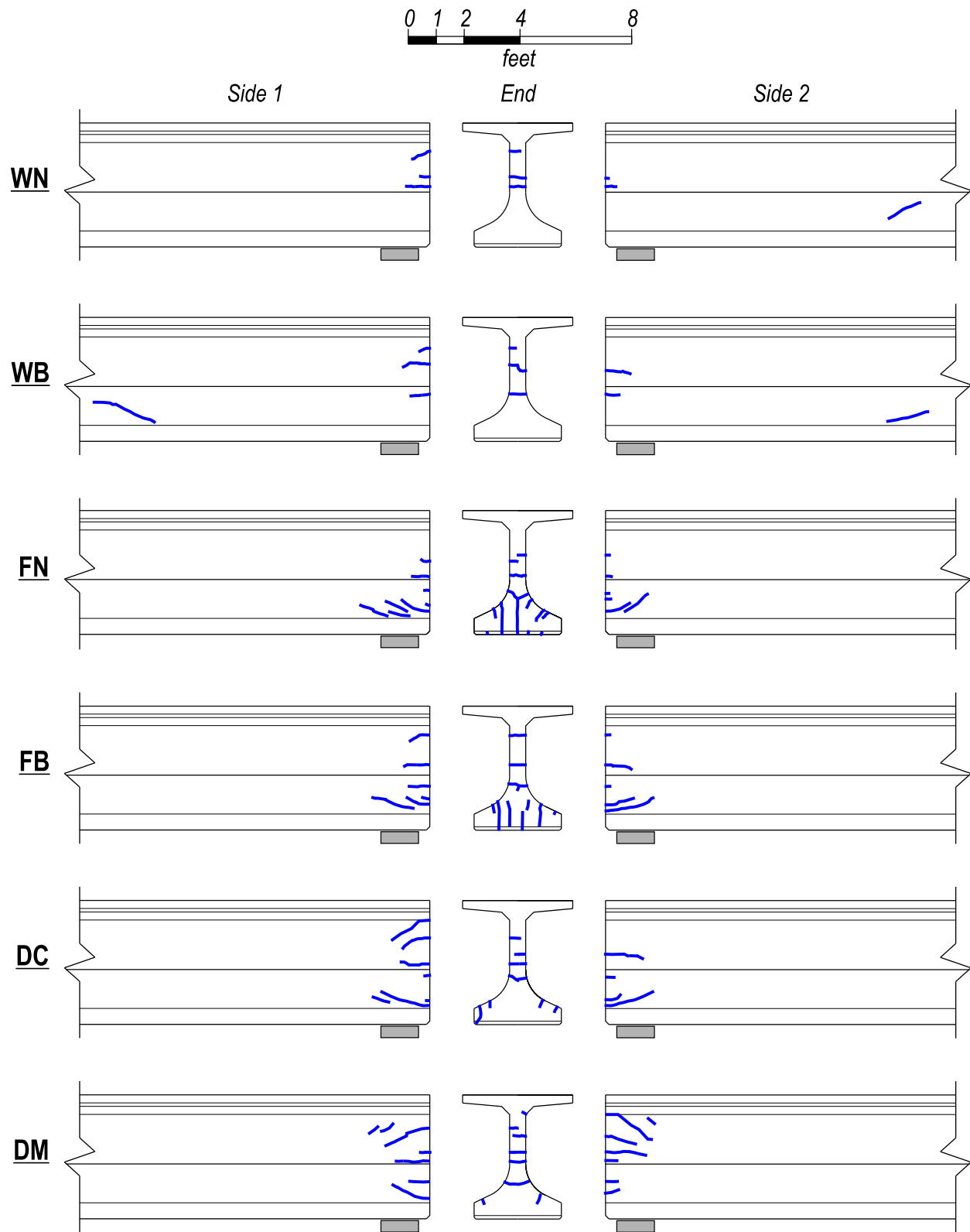
Figure 24–Girders W, F, & D web and flange splitting cracks
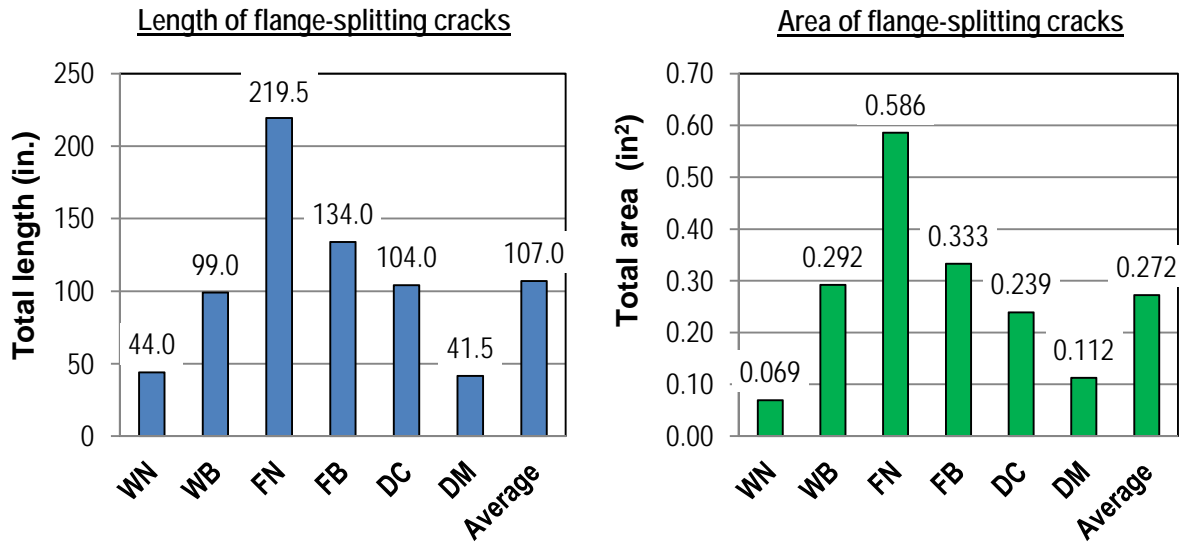
Figure 25–Flange splitting cracks girders W, F, and D

Figure 24 and Figure 25 demonstrate that variation in end region detailing can have a significant effect on the extent of cracking in the bottom flange and web. The effects of specific detailing schemes are discussed in greater detail in Appendix D.

One typical observation among most specimens was the formation of a flange splitting crack that intersected the outermost strand in the third row (Figure 26). This strand had the least amount of clear cover of any strand. Cracks at this location are attributed to the relatively small cover distance. Removing this strand from the pattern may reduce the potential for cracking.

5.2.3   Load Testing

Each specimen was load tested using the test setup shown in Figure 20. Maximum shear forces supported by the specimens and associated failure modes are presented in Figure 27. Forces include applied load and self-weight. End region detailing had significant effect on shear capacity. Specimen HC supported the largest shear force of 793 kip, almost twice as much as specimen FN which had a capacity of 402 kip. Experimental shear strength was increased by confinement reinforcement, bearing plates, and increased quantity of bonded prestressing strands. Strength was decreased when all fully bonded prestressing strands were placed in the outer portions of the bottom flange.
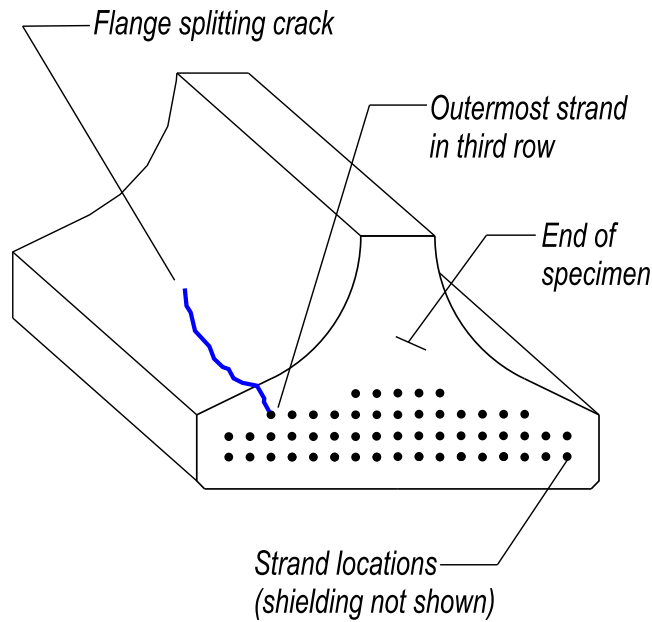
Figure 26–Typical flange splitting crack location
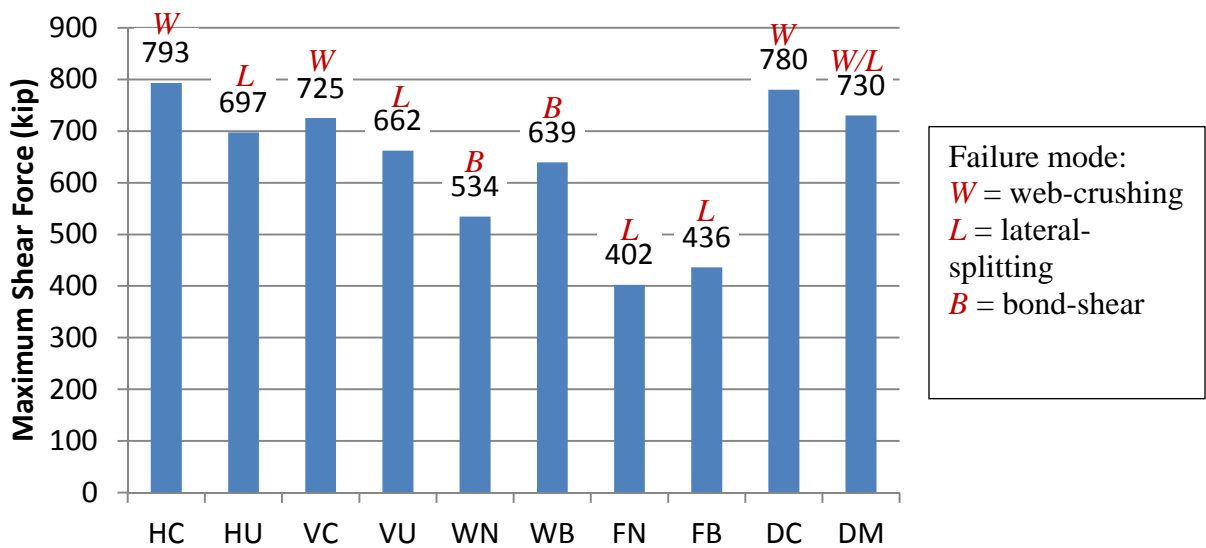
Figure 27–FIB-54 Peak shear forces

Three distinct failure modes were observed: Lateral-splitting failure, bond-shear failure, and web-crushing failure. Lateral-splitting failure occurred due to transverse tensile forces in the bottom flange (Figure 28). Longitudinal cracking through the bottom flange was characteristic of girders failing in lateral-splitting (Figure 3). Bond-shear failure (Figure 29) occurred when cracks formed within the development length of the prestressing strands, thereby interrupting

force transfer between the strands and concrete. Web-crushing failure occurred when diagonal compressive stresses exceeded the strength of the concrete in the web (Figure 30).

Lateral-splitting and bond-shear failures are considered "premature" failure modes because they occur prior to a girder reaching the desired web-crushing capacity. ACI 318 and AASHTO LRFD provisions for shear design both consider web-crushing failure. In the test program, lateral-splitting failures occurred in specimens lacking confinement reinforcement and in specimens with all fully bonded prestressing strands placed in the outer portions of the bottom flange. Bond-shear failure was observed in specimens with the smallest quantity of fully bonded strands.

Isometric
End region
& lateral-splitting crack

Section A-A
Without confinement
reinforcement

Section A-A
With confinement
reinforcement
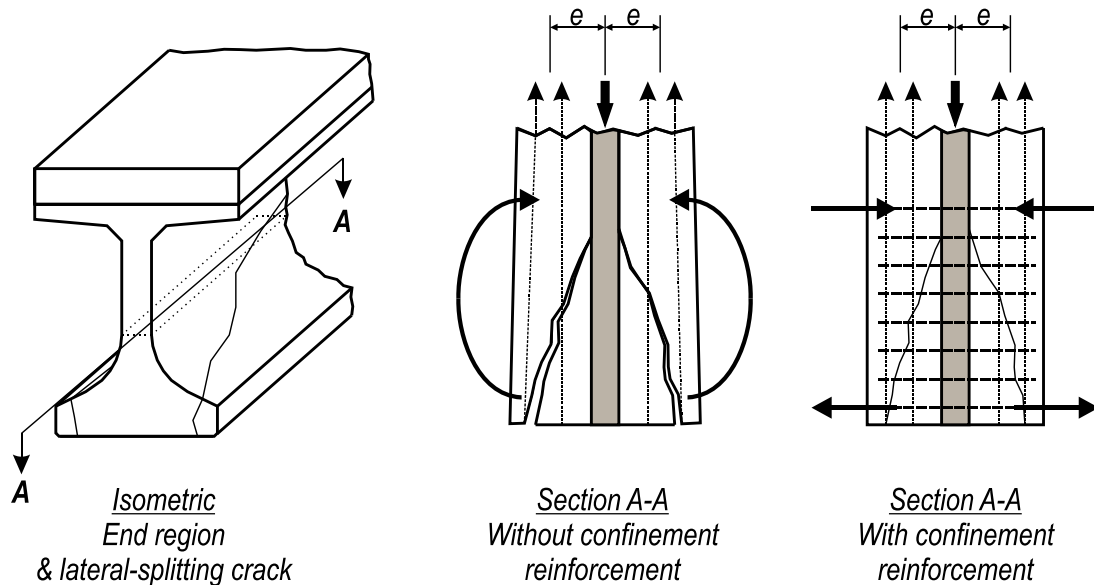
Figure 28–Lateral-splitting failure mechanics

A)   B)
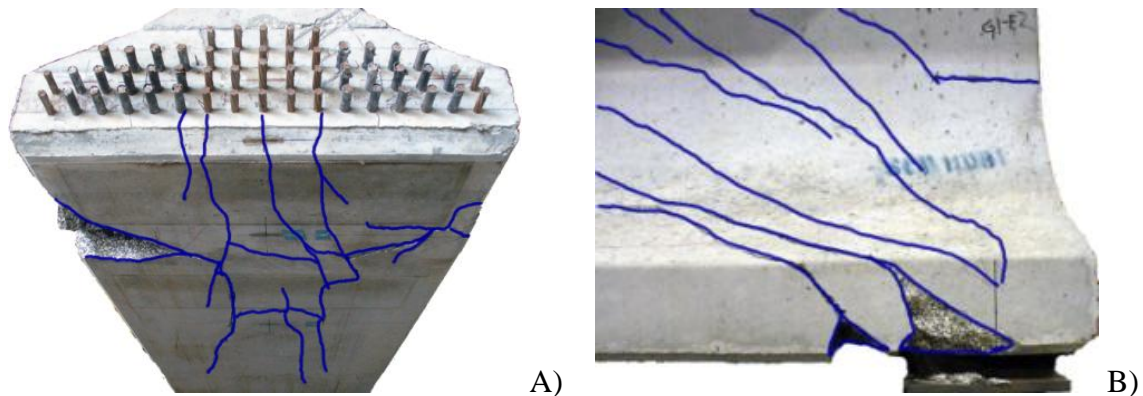
Figure 29–Bond-shear failure A) bottom view and B) side view

Figure 30–Web-crushing failure

Strain data from the confinement reinforcement and bearing plates were collected during load testing and were used to estimate the transverse forces acting in the bottom flange. Confinement and bearing plate forces are shown in Figure 31 for specimens HC and VC. Forces in the figure were calculated using strain data from ultimate load. Similar calculations were made for all test specimens. Results of these calculations suggest that significant (up to 100 kip) transverse forces were present in the bottom flange. These forces were carried by the confinement reinforcement and where present, embedded steel bearing plates.
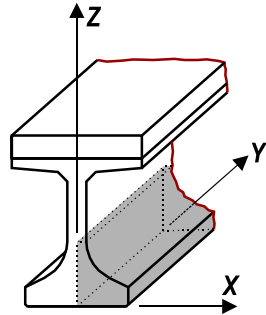
End region
isometric view

Bottom flange section
end view

$F_{CRx} = F_{CRx1} + F_{CRx2} + F_{CRx3}$

$\Sigma^- F_{CRx} = -25.7\ kip$

$F_{PLx} = -69.6\ kip$
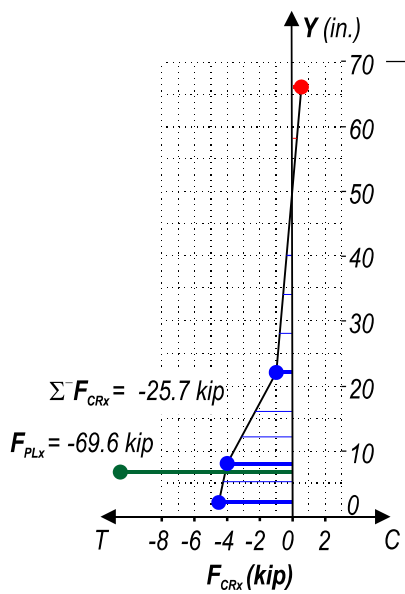
Bottom flange forces
specimen HC

$\Sigma^- F_{CRx} = -30.3\ kip$

$F_{PLx} = -70.1\ kip$
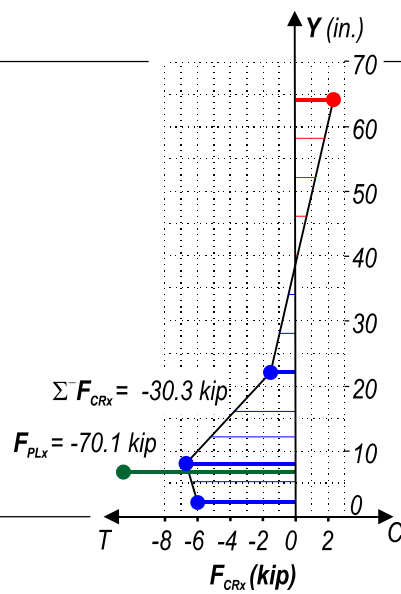
Bottom flange forces
specimen VC
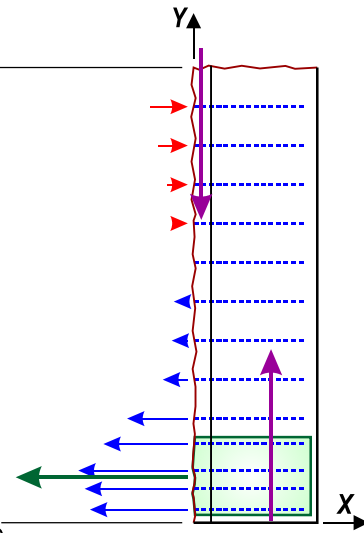
Bottom flange section
partial plan view

Figure 31–Transverse forces in confinement reinforcement and bearing plates

5.3   Conclusions

Ten uniquely detailed FIB-54 specimens were fabricated and tested to evaluate the effects of end region detailing on girder serviceability, behavior, and cracking. Variables in the test program included:

- Presence/absence of confinement reinforcement
- Quantity and configuration of confinement reinforcement

- Presence/absence of horizontal reinforcement
- Quantity of vertical reinforcement
- Presence/absence of embedded steel bearing plates
- Strand quantity
- Strand placement

The following is a partial list of conclusions. Additional conclusions and justifications are presented in Appendix D along with a more comprehensive presentation of test program results.

- Transverse tensile strains were measured in the bottom flange, confinement reinforcement and embedded bearing plates during and after prestress transfer. Tensile strains are attributed to a combination of prestressing forces, the Hoyer effect and girder self-weight and are thought to have caused flange splitting cracks.

- Transverse tensile strains are greatest in sections with fully bonded strands placed only in the outer portions of the bottom flange. Bonded strands in the outer flange are eccentric with the resultant internal force, thereby inducing bending in the bottom flange and associated transverse tension at the girder end.

- Differences in detailing have significant effect on end region cracks occurring due to prestress forces. All test specimens used the FIB-54 cross-section, yet the summation of end region crack lengths varied from a maximum of 291 in. to a minimum of 75 in.

- Flange splitting cracks extended up to 30 in. from the test specimens ends. This length is comparable to the AASHTO LRFD transfer length of 36 in. (60 strand diameters) suggesting that this is a reasonable extent for the placement of confinement reinforcement to control flange splitting cracks.

- Splitting cracks in the bottom flange typically intersected the outermost strand in the third row from the bottom. This strand location had the least amount of top cover of any location in the test girders.

- Differences in detailing, such as confinement reinforcement configuration, steel bearing plates, and strand pattern have significant effect on the end region capacity, even for members having the same cross-section. All test specimens used the FIB-54 cross-

section, yet experimental capacities ranged from a maximum of 793 kip to a minimum of 402 kip.

- Test specimens with confinement reinforcement detailed according to current FDOT specifications failed in web-shear mode and at an average load 13% higher than comparable specimens without confinement. Specimens without confinement failed in lateral-splitting.

- Current shear and longitudinal tie provisions resulted in nominal capacities that were unconservative (up to 32% too large) relative to some experimental capacities. Nominal capacities were unconservative in specimens without confinement reinforcement (HU), specimens without steel bearing plates (WN, FN), and specimens with bonded strands concentrated in the outer flange (FB, FN).

6 FIB-63 Tests

Web cracking at the end of the girder during and after prestress transfer is an ongoing problem for pretensioned concrete I-girders. The FIB-63 test program compared four different detailing schemes for controlling and/or preventing web cracking. Schemes include: current Florida Department of Transportation standard detail, 1-in. diameter vertical end zone reinforcement, vertical post-tensioning of the end region prior to prestress transfer, and partial debonding of 45% of prestressing strands. One scheme was implemented on each end of two 63 in. deep Florida I-Beams (FIB-63). Crack locations, lengths, and widths were monitored during prestress transfer, as well as during the weeks and months following transfer. Crack data were used to compare the relative effectiveness of each scheme in controlling web cracking. After crack data were collected and analyzed, each specimen was load tested to determine the effect of the detailing schemes on ultimate load. A more comprehensive presentation of the FIB-63 test program is presented in Appendix E.

6.1 Specimen Details and Test Setup

Two 50 ft. long FIB-63 girders were fabricated and tested for this program. Each end of each girder had unique end region detailing (Figure 32), which results in four different test specimens. Specimen CT served as the control specimen and followed current Florida Department of Transportation (FDOT) details (2010). Vertical end zone reinforcement in CT consisted of (16) #5 bars placed within 16.5 in. of the member end.

Specimen SL had the same end region reinforcement as specimen CT. Strands in SL, however, were 45% partially shielded. This percentage of shielded strands violated AASHTO LRFD requirements.

The end of specimen PT was vertically post-tensioned prior to prestress transfer. The post-tension force was designed to counteract vertical tensile stresses in the web. A post-tension force of 78 kip was applied by tightening nuts on six threaded rods placed in the end region. The area of end region vertical reinforcement was reduced by 33% relative to CT. The post-tension concept used in specimen PT was proposed by the FDOT structures design office.

The fourth and final specimen, LB, had 1-in. diameter threaded rods as vertical end reinforcement. Because it used larger reinforcement, LB had 30% more end reinforcement than CT. Specimen LB was located on the same girder but opposite end as specimen PT.

FIB-63 specimens were built at the same time as the phase 2 specimens from the FIB-54 test program. They were built by Standard Concrete Products of Tampa, FL. Photos of the test specimens during construction are shown in Figure 33
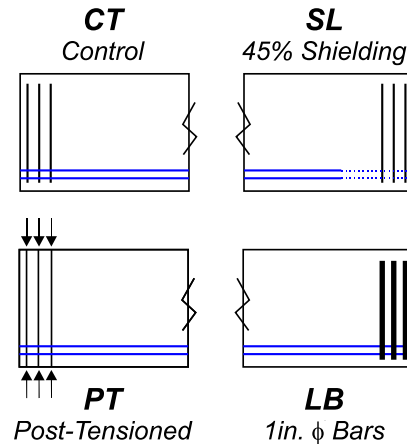
Figure 32–FIB-63 test specimen labels

Strain, crack, and material property data were collected during fabrication. Vibrating wire and electrical resistance strain gages were used to collect strain data. Crack data were collected using a tape measure and microscope. Material property data were collected for concrete compressive strength, reinforcement yield strength and elongation, prestressing strand strength, and prestressing strand bond capacity. The Standard Test for Strand Bond (NASP 2009) was used for determining strand bond capacity.

After fabrication, girders were trucked to the FDOT M.H. Ansley Structures Research Center in Tallahassee, FL for load testing. Each end (specimen) was loaded in 3-point bending as shown in Figure 34. After the first end was tested, the load point and supports were move and the opposite end was tested. Load, displacement, strain, and strand-slip data were collected during load testing.

<center>Specimen CT   Specimen SL</center>

<center>Specimen PT   Specimen LB</center>

<center>Figure 33–FIB-63 test specimens during construction</center>
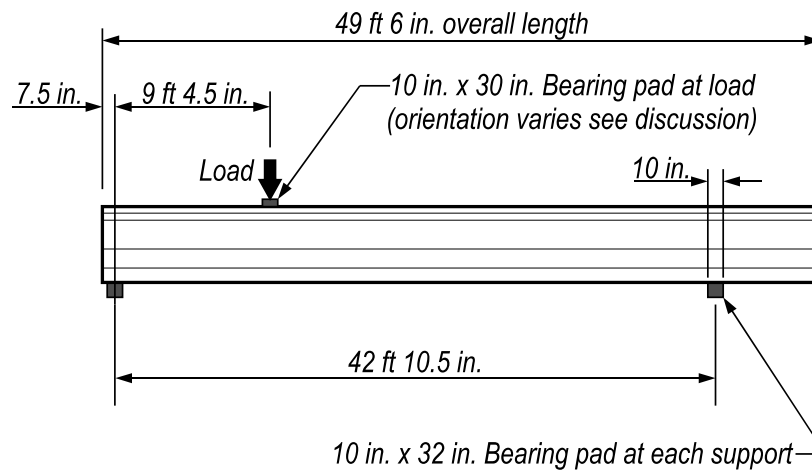
<center>Figure 34–FIB-63 test setup</center>

Orientation of the bearing pad at the load point varied. Specimen LB was tested first and had the pad oriented such that the 30 in. dimension was perpendicular to the span length. This led to failure in top flange, and the pad orientation was rotated 90 degrees for the subsequent tests.

6.2 Results and Conclusions

6.2.1 Cracks due to Prestress

Cracking in the end region was monitored during prestress transfer and in the weeks and months following transfer. Figure 35 shows the formation and growth of cracks in the control specimen. Similar figures are shown for the other specimens in Appendix H. Cracks were first observed during prestress transfer and grew in length and quantity in the months following prestress transfer. Load tests were conducted approximately four months after transfer. Photos of the specimens are shown in Figure 36.

Crack data are quantified in Figure 37 and Figure 38. Data presented in these figures were used to compare the relative effectiveness of the different detailing schemes in controlling web cracks. Based on the metrics of total length and total area, the control detail (specimen CT) was the least effective in controlling web splitting cracks. Specimen CT at had 28% more length and 53% greater area than the average of all specimens.

Specimen SL was the most effective detail according each metric except total length. SL had 59% less area, and 44% smaller average width than the control specimen. The reduction in crack length, area, and width observed in specimen SL is attributed to the partial strand debonding which reduced tensile stresses in the end region.

In terms of crack length, the post-tensioning detail of specimen PT was the most effective for controlling web splitting cracks. Web splitting crack length in specimen PT was 50% less than the control specimen. Figure 36 shows that the post-tensioning effectively mitigated all web cracks at the end surface of the member. Web cracking did, however, occur away from the end surface.
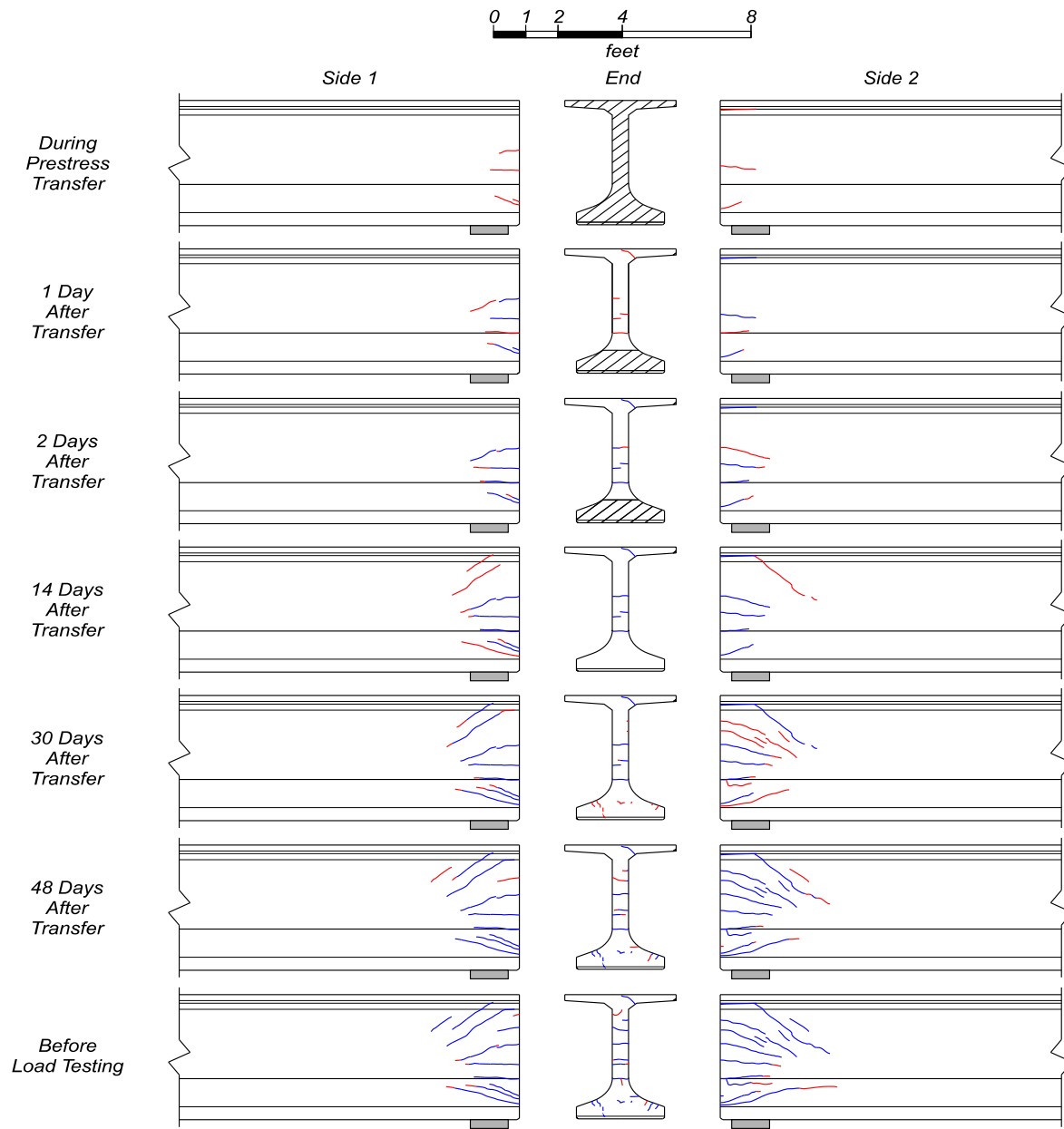
Figure 35–Crack growth in specimen CT (flexural cracks in top flange not shown)
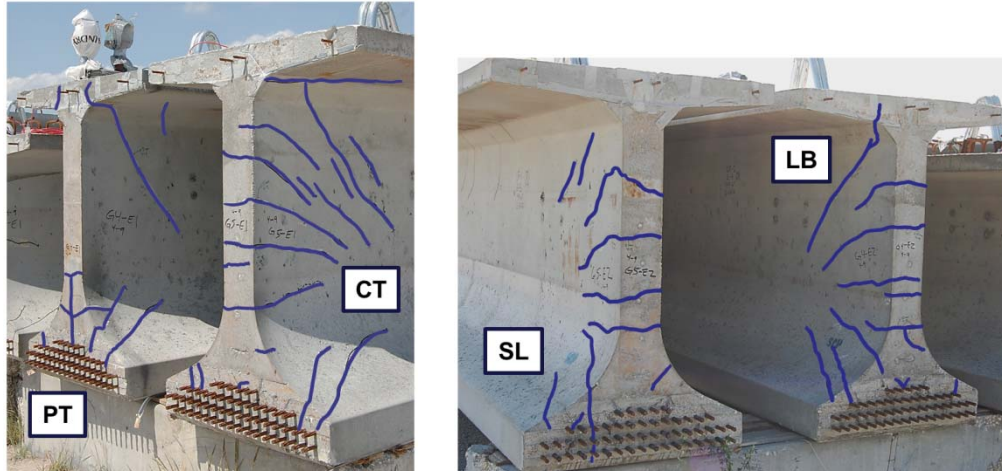
Figure 36–Photo of FIB-63 end region cracks (cracks enhanced in blue)

Web cracks away from the end of specimen PT extended diagonally into the web from the post-tensioning anchor plate. Forces introduced at the plate are believed to have contributed to the formation of the diagonal cracking in specimen PT. The diagonal web crack in PT had the greatest web crack width and the largest average web crack width (~0.006 in.), which was 30% greater than that of the control specimen.

Detailing of specimen PT had a negative effect on the bottom flange spitting cracks. Referring to Figure 36, it can be observed that PT was the only specimen to have a vertical splitting crack on the end surface. This crack is attributed to development of the post-tensioning rods in the bottom flange.

Specimen LB performed better than the control specimen in every metric except maximum crack width. Specimens LB and CT had the same maximum crack width of 0.008in. For LB, the total web crack length was 10% smaller and the average web crack width was 35% smaller than in the control specimen.
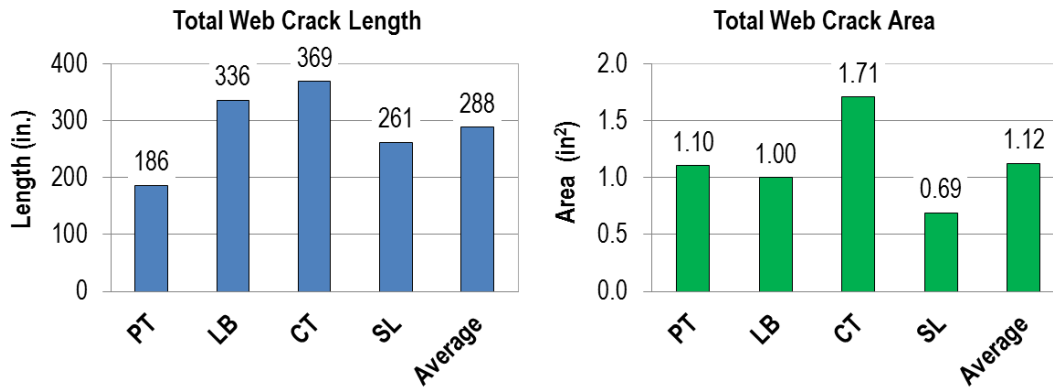
Figure 37–Web splitting crack length and area
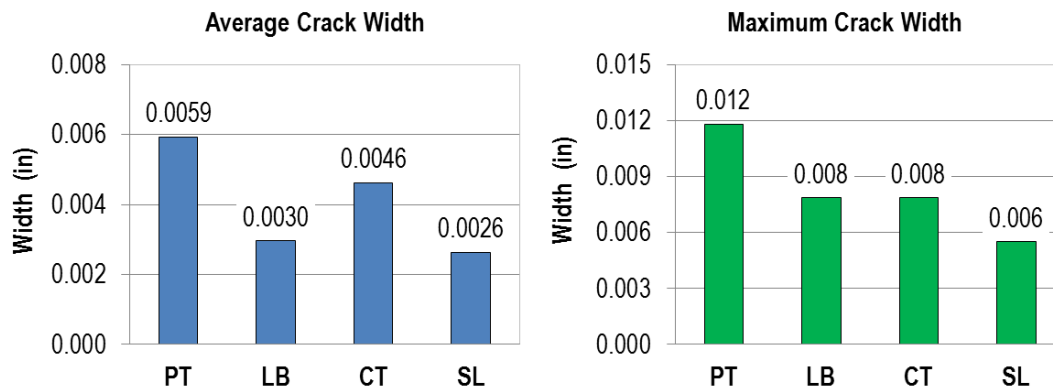
Figure 38–Web splitting crack widths

6.2.2 Load Tests

Specimens were load tested using the setup shown in Figure 34. Specimen LB was first to be tested. The primary variable in LB was the use of eight 1-in. diameter threaded rods as end region vertical reinforcement. LB supported a maximum shear force of 612kip. Peak load was controlled by a punching failure through the flange (Figure 39), which was caused by the orientation of the bearing pad at the load point. Pad orientation was rotated 90 degrees in subsequent tests to prevent this failure mode. Effect of end region detailing in LB on shear capacity could not be determined because of the punching failure in the top flange. In spite of the undesirable failure mode, LB still exhibited capacity that was approximately 20% greater than the code-calculated nominal shear capacity.
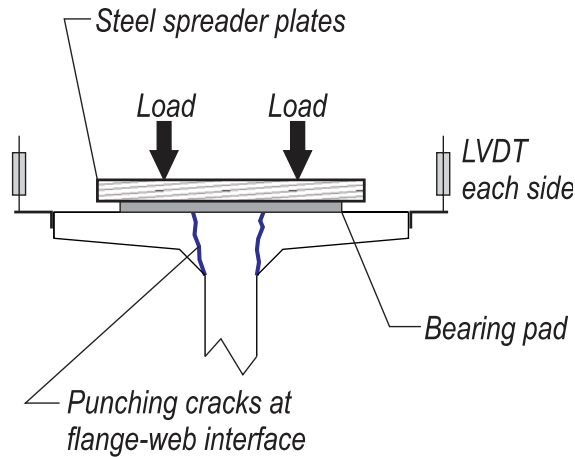
Figure 39–Punching failure specimen LB

The control specimen (CT) supported a maximum shear force of 791 kip. Peak load was controlled by failure of the web (Figure 40). After testing it was observed that the top hooks of the vertical reinforcement experienced breakout failure due to lack of sufficient cover (Figure 41). Top hooks from the vertical reinforcement were embedded in the relatively thin top flange because a topping slab was not cast on the specimen. It is not known if the hook failure precipitated or was a by-product of the web failure. The bearing pad at the load point also punched through the top flange at peak load (Figure 41). Capacity of CT exceeded the code-calculated nominal shear capacity by approximately 50%.

Specimen SL supported a maximum shear force of 609 kip, which is the smallest of any FIB-63 specimen. The primary variable in specimen SL was partial strand shielding of almost half of the prestressing strands. Failure of SL was categorized as a bond-shear failure. The reduced number of fully bonded strands in SL was culpable for the bond-shear failure and lower capacity. Specimens CT, LB, and PT had almost twice as many bonded strands and were less affected by cracks interrupting the strand development length. As such bond-shear failure did not occur in these other specimens.

Specimen PT supported a maximum shear force of 800 kip. The primary variable in PT was the presence of vertical post-tensioning in the end region. The capacity of the testing equipment was reached prior to failure occurring in specimen PT. As such, the controlling failure behavior could not be determined. Based on comparison with the control specimen (CT) it can be concluded that the end region post-tensioning did not adversely affect the shear capacity of specimen PT.
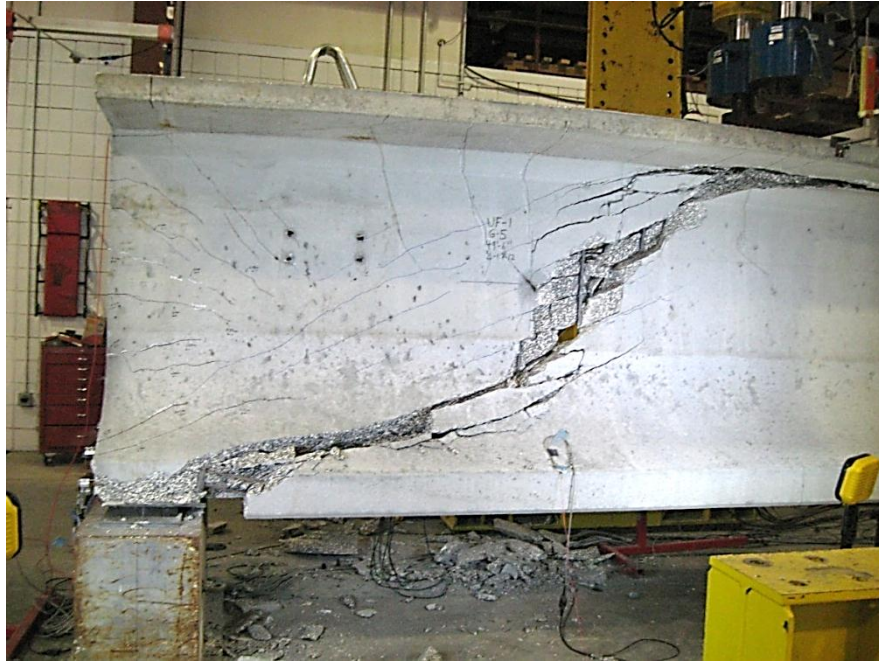
Figure 40–Specimen CT after load tests
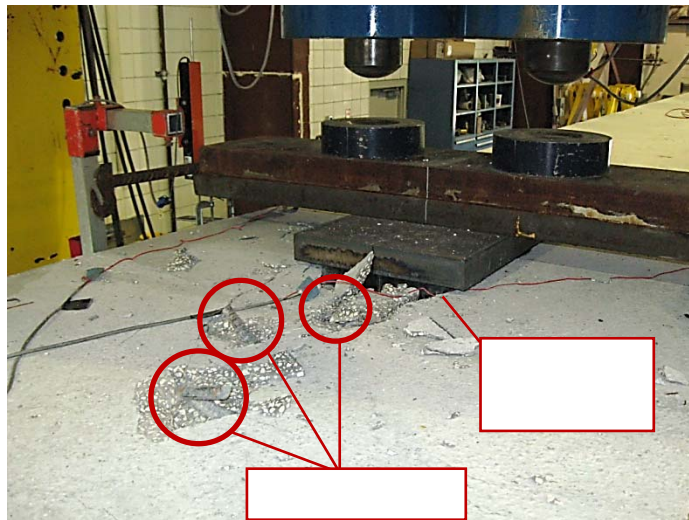
Figure 41–Hook breakout and load point punching failures

6.3   Conclusions

Four FIB-63 test specimens were fabricated and load tested to evaluate the effects of different end region detailing schemes on the control of web splitting cracks. Details in the test program included: 1) #5 vertical end region reinforcement per current FDOT standards (control specimen), 2) vertical reinforcement per FDOT and 45% partial strand shielding, 3) vertical end region post-tensioning, and 4) 1 in. diameter threaded rods as vertical reinforcement. Cracks and

strains were monitored during prestress transfer and in the weeks following transfer. These data were used to compare the relative effectiveness of each detailing scheme in controlling web splitting cracks. Finally, specimens were load-tested in 3-point bending to determine what, if any, effect the end region detailing had on shear capacity and behavior. Key observations and conclusions are as follows:

- Partial strand shielding was an effective means of controlling the length, and width of web splitting cracks. Of the 52 strands in specimen SL 45% were shielded within the end region. Shielding resulted in a 29% reduction in web crack length and a 43% reduction in average web crack width relative to the control specimen.

- Vertical post-tensioning of specimen PT prevented web splitting cracks at the end surface, but affected other web cracks away from the end and in the bottom flange. The largest web cracks in the test program occurred in specimen PT.

- All web cracks in the test program had widths equal to or less than 0.012in. Cracks above this width require corrective action based on FDOT requirements for moderate environments.

- Increasing the end region vertical reinforcement decreased the length and width of web splitting cracks. Specimen LB had 30% more vertical end region reinforcement than the control specimen, and had 10% less web crack length and 35% lower average web crack width.

- Experimental capacity of all specimens was greater than the ACI 318 and AASHTO LRFD calculated nominal shear capacities.

- Increased strand shielding in specimen SL resulted in a reduction in the experimental capacity of specimen SL. Because of strand shielding this specimen had insufficient fully bonded strands to prevent bond-shear failure after cracks formed in the above flange in front of the bearing.

- Vertical post-tensioning in the end region of specimen PT did not affect load capacity. Specimen PT supported the largest load of any specimen. Failure of PT could not be reached due to limitations of the testing equipment.

- Specimen LB experienced a punching shear failure in the top flange due to placement of the applied load. Consequently, the effect on load capacity of

increased vertical reinforcement (relative to the control) in specimen LB could not be evaluated. It is assumed that the additional vertical reinforcement would not have had negative effect.

7   Finite Element Analyses of End Region

FE (finite element) modeling was conducted to evaluate the behavior of the end region during prestress transfer and under applied loads. The FEA (finite element analysis) program Adina (2009) was used to conduct all modeling and analysis. All models were linear elastic and were intended to model the girder behavior prior to cracking. Strain gage and displacement data from the Small Beam and FIB-54 test programs were used to validate the FE models. The validated models were then used in parametric studies to evaluate variables that were not included in the experimental programs. A summary of the analyses are presented in this section. A more comprehensive presentation of the FE modeling is contained in Appendix F.

7.1   Analyses at Prestress Transfer

7.1.1   Model Configuration and Validation

Girder behavior during prestress transfer was evaluated using the FE model configuration shown in Figure 42. The end region was modeled with 27-node 3D solid elements. Beam elements were used away from the end region to reduce computation demand. Transition for solid element to beam elements was achieved using rigid shell elements and links. The FE model was linear-elastic and was intended to model end region behavior prior to cracking.

Prestressing forces were applied as point loads to nodes occurring at strand locations. Prestressing forces were applied over a transfer length of 17.5 in. from the member end. Only the prestressing forces were considered in the model, strands were not explicitly modeled. Loads, boundary conditions, and girder geometry were symmetric about the Z-Y axis as shown in Figure 42. This allowed for use of a half-symmetry model to reduce computation demand.

One critical feature of the model was that prestressing forces were applied sequentially as occurs in physical girders during prestress transfer. To match the transfer process used in the experimental programs, prestressing forces were applied from the outside-in. In this manner the stress and strain state of the end region could be evaluated at different stages of the prestress transfer process. Self-weight was applied using the 'mass proportional' load feature of ADINA.
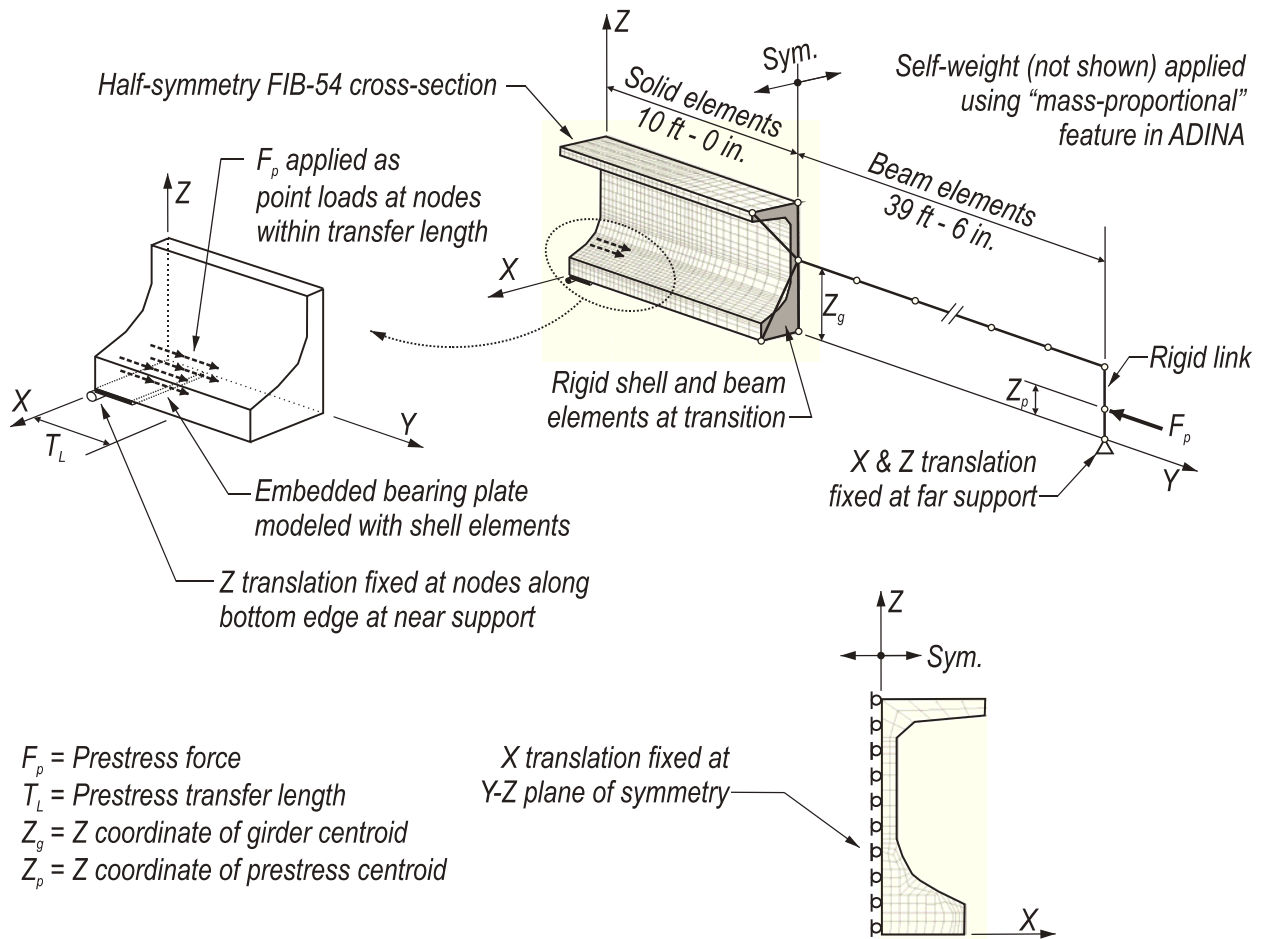
Figure 42–FE model details

The model configuration shown in Figure 42 was validated using experimental data from the FIB-54 test program. Two stages of prestress transfer were considered in the validation. Stage 1 corresponded to the condition when only the strands in the outer portions of the bottom flange had been released. Stage 2 corresponded to all strands being released. Partial results from the validation study are presented in Figure 43. In general the FE model did an excellent job of capturing the strain behavior at both of the stages considered. A mesh convergence study was also conducted to verify the adequacy of the mesh density. Based on the convergence study a mesh density of 2 in. was deemed adequate for the modeling conducted.

Figure 43–Comparison of experimental and FE model transverse (x-x) strain

7.1.2 Parametric Studies

After validation and verification the model shown in Figure 42 was used to conduct parametric studies of end region behavior during prestress transfer. Parameters included: stages of prestress transfer, steel bearing plates, and transfer length. Studies were also conducted to quantify the transverse stresses and forces at different locations in the bottom. Forces were calculated by integrating stresses over the section of interest as shown in Figure 44. Additional details of the integration procedure are presented in Appendix F.
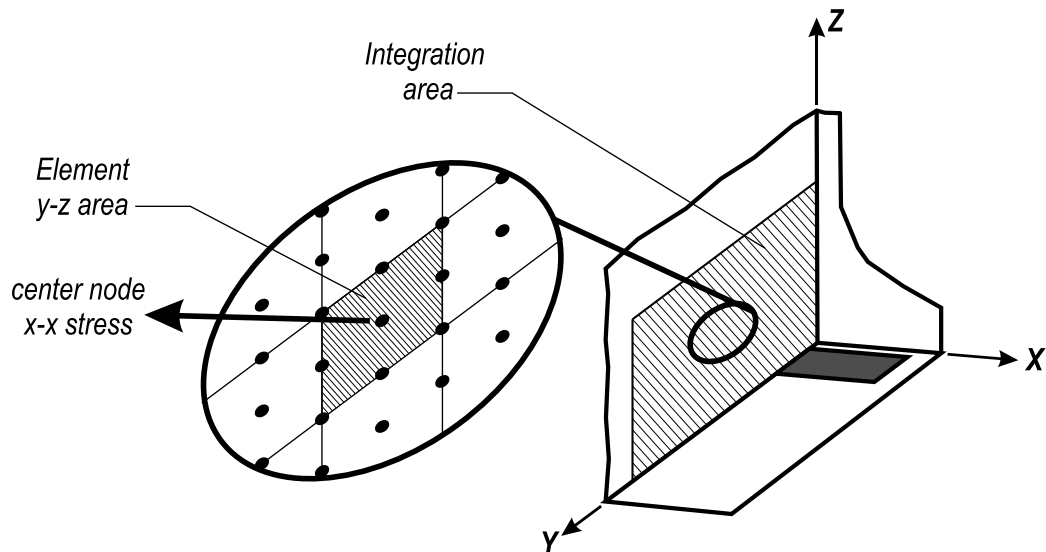
Figure 44–Element x-x stress and y-z area

Results of the strand release parametric study are presented in Figure 45 and Figure 46. In this study prestress forces were sequentially added to the model from outside-in, mimicking the prestress transfer process used in the experimental programs. The horizontal axis of Figure 46 is the percentage of the strands released at a given stage. The vertical axis is the normalized transverse tensile force occurring in the bottom flange above the bearing. Transverse force was obtained by integrating stresses such as those shown in Figure 45. Results indicate that the transverse force is greatest when only the outer strands are cut.
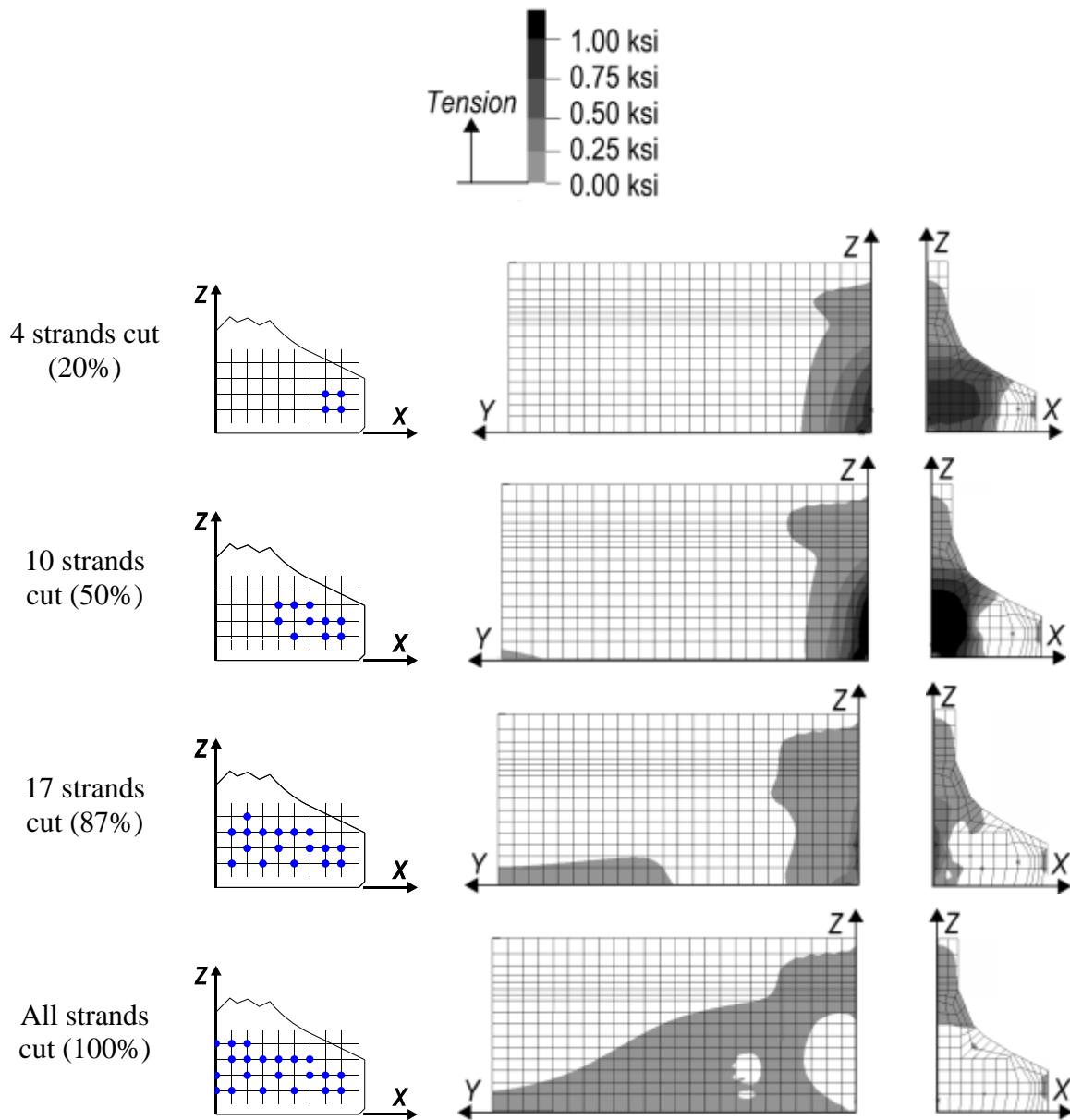
Figure 45–Transverse (x-x) stress at stages of prestress transfer
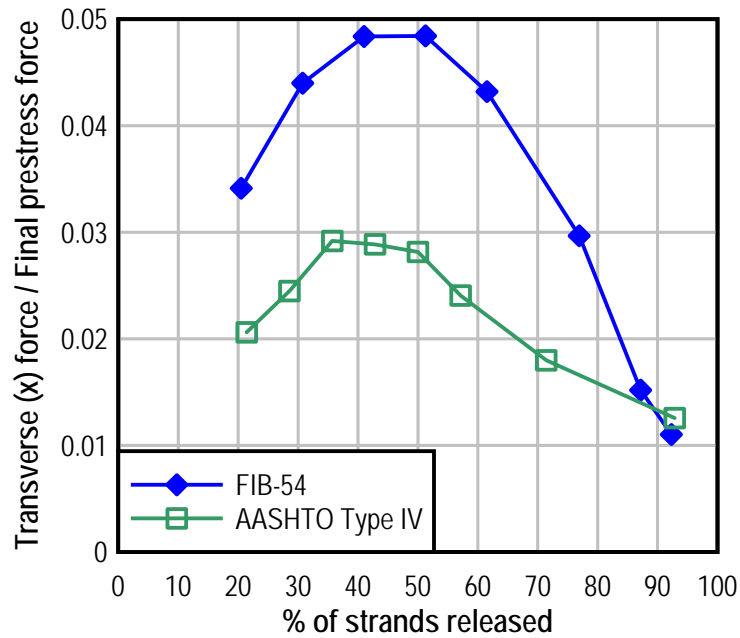
Figure 46–Transverse force variation as strands are released

Effects of transfer length were also studied by varying the length over which prestress forces were applied to the FE model. For each transfer length considered, the transverse force in the bottom flange was quantified using the procedures discussed previously in this section. Figure 47 shows that transverse tensile force in the bottom flange has an inverse linear relationship with transfer length. Shorter transfer lengths create the largest transverse forces.
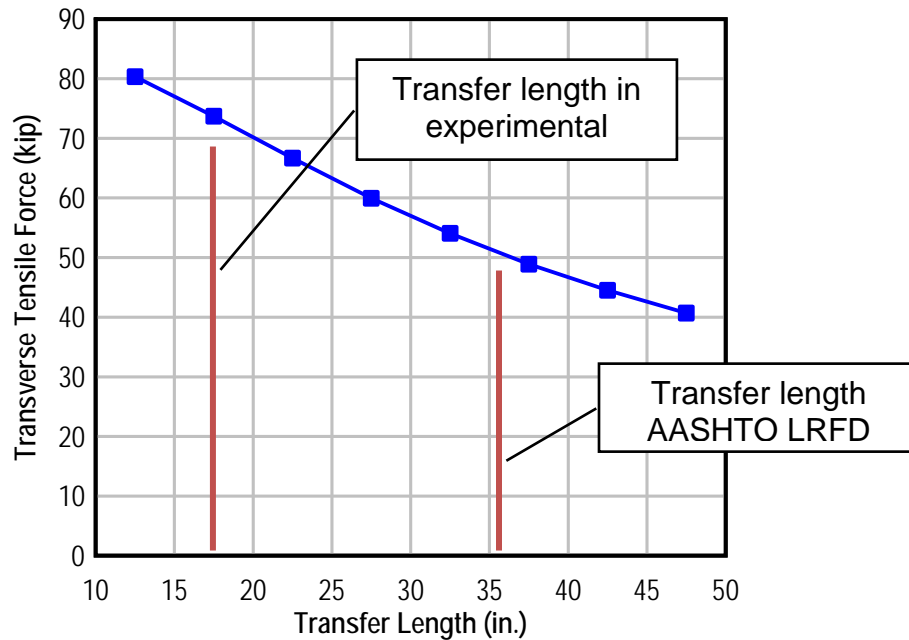
Figure 47–Transverse force variation with length of prestress transfer

7.2 Analyses during Loading

7.2.1 Model Configuration and Validation

End region behavior under applied loads was analyzed using the model shown in Figure 48. This model was similar to the one used to study behavior during prestress transfer (Figure 42), but had specific features to represent girders during load testing. Boundary conditions during the test programs consisted of reinforced neoprene bearing pads. This condition was modeled using a bed of spring elements spread over the bearing pad area. Girders in the test programs were loaded using hydraulic actuators acting on the top flange. This condition was modeled as a pressure load acting over an area similar to the load point in the test specimens.

The FE model was validated using data from the small beam test program. Partial results from the validation study are shown in Figure 49, which compares experimental strain data (black diamonds) with the strain calculated using the FE model. As shown in the figure, the FE model was in good agreement with the experimental data. A mesh convergence study was also conducted to verify the adequacy of the mesh density. Based on the convergence study, a mesh density of 1 in. was deemed adequate for modeling specimens from the small beam test program.
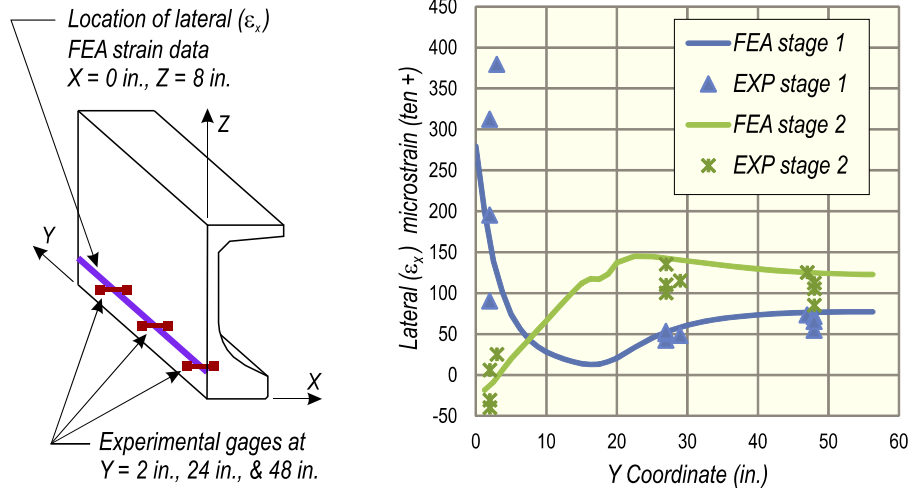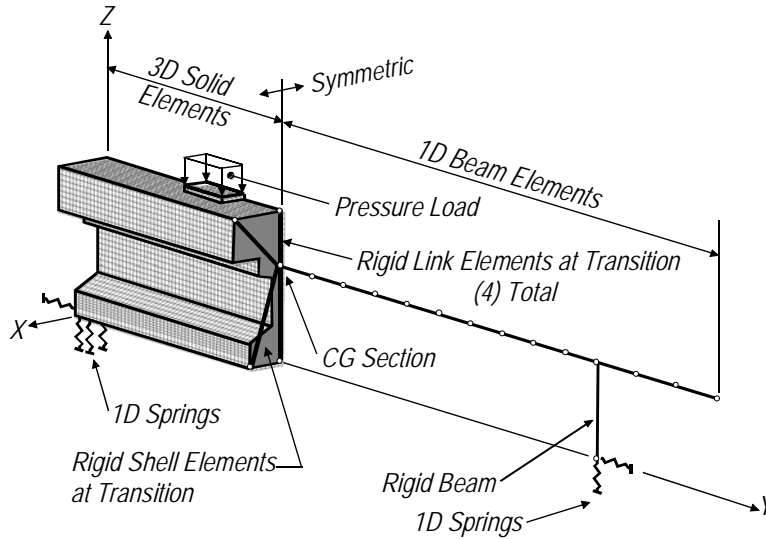
Figure 48–FE model configuration
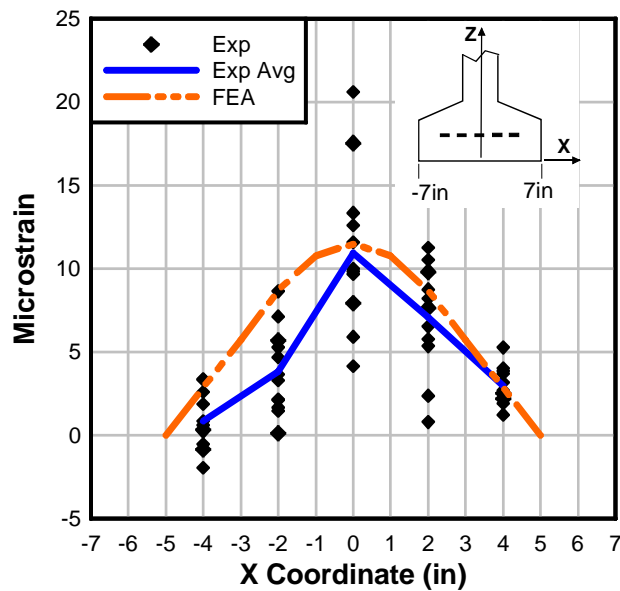
Figure 49–Small beam transverse (x-x) strain profile (V = 15 kip)

7.2.2   Parametric Studies

After validation and verification the model shown in Figure 48 was used to conduct

parametric studies of end region behavior during loading. Parameters included: bearing pad

width, bearing pad stiffness, and presences of steel bearing plates. Results of the study on

bearing pad width are shown in Figure 50. The figure shows how the transverse strain changes

as a function of the bearing width. When the bearing width is narrow (relative to the flange) the

maximum strain occurs at the mid height of the bottom flange. When the bearing width was wide the maximum strain occurred at the bottom of the bottom flange. Based on the parametric study it was determined that transverse strain in the bottom flange can be minimized when the bearing pad width is approximately 60% of the flange width. Narrow bearing widths, however, may adversely impact the stability of the girder during construction.
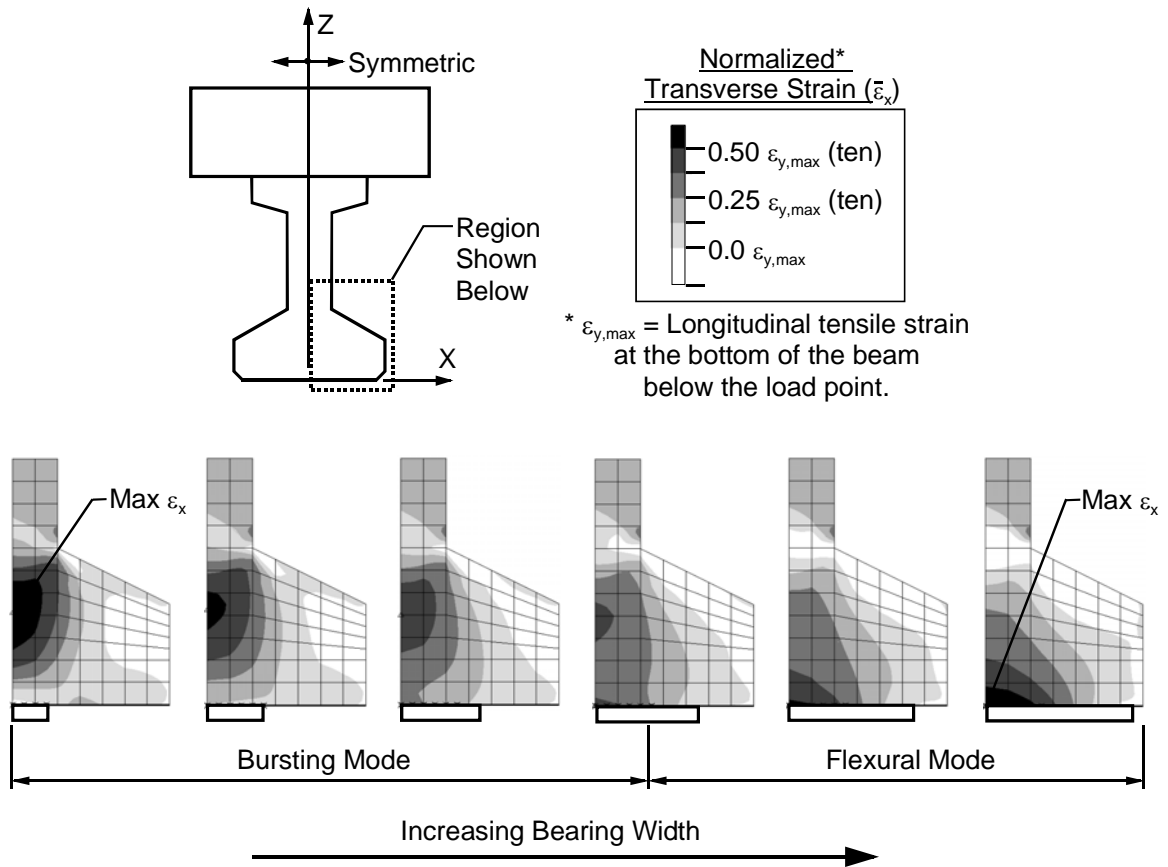
Figure 50–Normalized transverse (x-x) strain vs. bearing pad width, small beam

7.3 Conclusions

Linear-elastic FE models were used to evaluate the effects of prestressing forces and applied loads on the behavior of I-girder end regions. Models were validated using experimental data and were verified through convergence studies. Analyses are discussed in greater detail in Appendix F. The following is a partial list of conclusions regarding behavior during prestress transfer:

- Embedded steel bearing plates carry transverse tension during and after prestress transfer. In the linear-elastic range, plates in FIB girders carry 10% of the tension force due to prestressing. Load testing indicated that the bearing plate carries a significantly greater proportion of the transverse tensile force at ultimate capacity. The portion carried by the plates does not vary during different stages of strand cutting.

- Transverse stress and forces are inversely proportional to strand transfer length. Thus the greatest transverse effects occur in girders with the shortest transfer lengths. A 50% reduction in transfer length causes an increase of approximately 50% in transverse tension.

- During prestress transfer, the maximum transverse tensile stress on an arbitrary vertical line through the bottom flange occurs when only the strands outboard (closer to edge) of the line have been cut. Cutting of strands along or inboard (closer to centerline) of a line relieve tensile stresses on that line.

- Self-weight reaction produces transverse tension forces in the bottom flange above the bearing. For Florida I-beams, the transverse tension force due to self-weight equals 28% of the reaction.

Conclusions were also made with regard to end region behavior due to applied loads:

- For the range of stiffness values reported for neoprene bearing pads, variations in pad shear stiffness have negligible effect ($< 0.1\%$) on the transverse strain in the end region. However, variations in pad axial stiffness can change the transverse strain by +/- 3%.

- Depending on the width of the bearing pad, two types of strain distributions (behaviors) occur in the end region of I-girders. A behavior denoted as 'bursting' occurred when the bearing pad width was narrow, and the transverse strain was distributed in a bottle-shaped manner. However, 'flexural' behavior occurred when the pad width was large, and transverse strain was dominated by flexural strains in the flange.

- The transition between 'bursting' and 'flexural' behavior occurred when the bearing pad width was approximately equal to 60% of the bottom flange width. This pad width also corresponded to the minimum transverse tensile strain.

- Steel bearing plates reduced the magnitude of transverse strain in the concrete adjacent to the plate, but the strain dissipates significantly with increasing distance from the plate. This effect was most pronounced when the bottom flange was acting in the 'flexural' mode.

- For the applied loads in the analytical study the transverse force in the bottom flange was approximately 25% of the reaction force.

8   End Region Design Models

AASHTO LRFD contains prescriptive requirements for the quantity and placement of confinement reinforcement located in the bottom flange of pretensioned concrete I-girders. A rational model for designing confinement reinforcement was developed as an alternative to the prescriptive requirements of AASHTO LRFD. The model considers a wide range of conditions and variations, yet is intended to be practical enough for use by bridge design engineers. The model is based on the ultimate strength limit state and specifically focuses on preventing lateral-splitting failures.

In addition to ultimate strength, serviceability of I-girder end regions must also be considered. Experimental and analytical research presented in previous sections has demonstrated that transverse tensile stress in the bottom flange of pretensioned I-girders can lead to flange splitting cracks during fabrication. A serviceability design model was developed for quantifying bottom flange splitting stress. Stress from the model can be compared to concrete tensile capacity to determine the likelihood of bottom flange splitting cracks.

Detailed derivations of the confinement reinforcement and serviceability models can be found in Appendix G.

8.1   Confinement Reinforcement Design Model

Experimental and analytical work from the previous sections has shown that confinement reinforcement carries transverse tension forces due to prestressing and applied loads. By carrying these forces the confinement reinforcement functions to prevent lateral-splitting failure and provides a normal force whereby strand tension forces can be transferred to the concrete after strut-and-tie behavior has initiated. The confinement reinforcement design model was created to address each of these functions. Forces generated due to these functions are referred to as the transverse tie force (F_{TTu}), and the strand anchorage force (F_{SAu}). An equation for calculating F_{TTu} was derived using strut-and-tie modeling:

$$F_{TTu} = R_u \left(\frac{n_f}{n_{strands}} \right) \left[\frac{(b_f - b_w)}{3t_f} - 3.1 \left(\frac{W_b}{b_f} \right) + 3 \right] \qquad \text{8-1}$$

Where:

R_u = Factored reaction force
n_f = Number of strands in the outer portion of the flange (Figure 51)
$n_{strands}$ = Total number of strands
b_f = Bottom flange width
b_w = Web width
t_f = Minimum thickness of bottom flange
W_b = Width of bearing pad
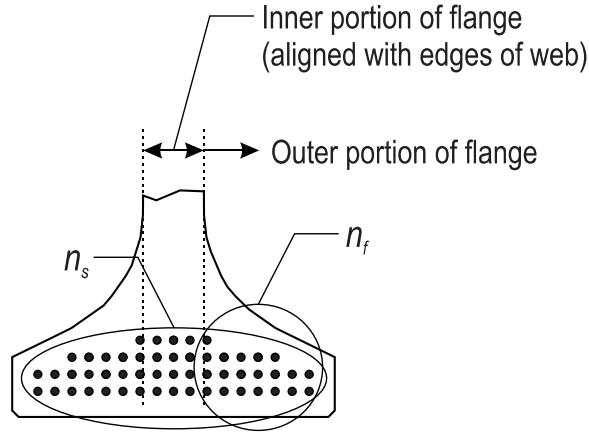
n_s = total number of fully bonded strands in bottom flange
n_f = number of fully bonded strands in outer portion of flange
(one side only)

Figure 51–Definition of number of strands in outer portion of flange n_f

An equation for F_{SAu} was derived using a shear-friction model:

$$F_{SA} = \frac{A_{ps} f_{pe} n_c}{\pi \mu}$$

8-2

Where:

A_{ps} = Cross-section area of all prestressing strands
f_{pe} = Effective prestress
n_c = Number of strands along critical section
μ = Coefficient of friction between concrete and strand, taken as 0.4

The model requires that the confinement reinforcement be designed for a factored tension force taken as the greater of F_{TTu} and F_{SAu}:

$$F_{CRu} = \text{maximum } (F_{SA}, F_{TTu}) \qquad\qquad 8\text{-}3$$

Where:

F_{CRu} =   Factored design force in confinement reinforcement

The quantity of confinement required at ultimate load is equal to the confinement reinforcement design load divided by the specified yield stress of the reinforcement:

$$A_{CR} = \frac{(F_{CRu})}{f_{yCR}} \qquad\qquad 8\text{-}4$$

Where:

A_{CR} =   Required area of confinement reinforcement

f_{yCR} =   Yield stress of confinement reinforcement

Results from the experimental program demonstrate that confinement reinforcement is most effective when placed near the end of the girder. As such, confinement reinforcement required by Equation 8-4 should be placed as close to the end of the girder as reasonable, but should also be placed over a distance of at least the transfer length.

Where bearing plates are provided the model allows the cross-sectional area of the bearing plate to account for up to 50% of the required confinement reinforcement.

The design model was compared to data from the small beam and FIB-54 experimental programs as well as to experimental results published in the literature. Figure 52 compares confinement reinforcement installed in each test girder with the required confinement reinforcement calculated using the proposed model (Equation 8-4). The factored reaction force used to calculate the transverse tie force (F_{TTu}) was taken as the nominal shear strength. Provided confinement reinforcement, plotted on the vertical axis, was taken as the area of confinement reinforcement placed within the transfer length. If present, the embedded steel bearing plate area was allowed to contribute up to 50% of the confinement requirement. Prestress losses were assumed to be 20 percent.
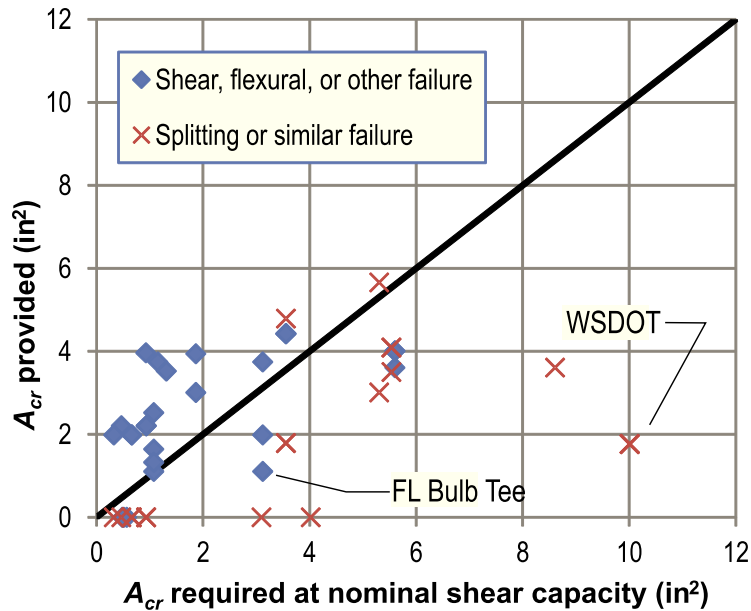
Figure 52–Design model compared to nominal strength of experimental girders

Points below the solid line have less confinement than calculated by the model, and were predicted by the model to fail due to splitting or lateral-bursting. The proposed model correctly identified all but two of the specimens that failed in lateral-splitting, bearing, or similar modes. Splitting and similar failures are denoted by the 'X' markers. The model incorrectly predicted failure in eight cases, as denoted by the diamond shaped markers below the solid line. In most cases where the failure mode was not accurately predicted, the provided confinement reinforcement was within 1.5 in^2 of the calculated requirement, indicating a desirable degree of conservatism in the model.

8.2   Serviceability Model

Experimental results from the FIB-54 and FIB-63 test programs demonstrate that splitting cracks can form in the bottom flange of I-girders due to prestressing forces. A model was developed for calculating tensile stresses that cause the flange splitting cracks. The following phenomena lead to transverse tensile stresses and are thusly considered in the serviceability model:

- Hoyer effect
- Eccentric prestress forces
- Self-weight reaction

Concrete stresses due to eccentric prestress forces are referred to in the design model as "peeling stress". This term was selected because the eccentric prestress forces act to "peel" the outsides of the bottom flange away from web (Figure 28). Concrete stresses due to the Hoyer effect are referred to as "Hoyer stress."

FE modeling (Appendix H) has shown that self-weight reaction stresses (due to Poisson's effect) at the end surface of FIB girders can be neglected at locations in the outer portion of the bottom flange. As such, stress due to self-weight was assumed to be zero for comparison of the serviceability model with experimental results from the FIB-54 and FIB-63 test programs. This assumption may not be reasonable for all cross-sections.

Vertical splitting cracks can occur at multiple locations in the bottom flange (Figure 53). Derivation of the serviceability model focused on splitting cracks through the outer portion of the flange. Bottom flange splitting cracks below the web were not considered because they are associated with extreme strand bond patterns that are not permitted in FDOT production girders.

An outside-in strand release pattern is commonly used in FDOT production girders. As such, this is the pattern considered in the serviceability model. The model does not apply to girders with other strand release patterns.

Two critical conditions (Figure 54) are considered in the design model:

- **Maximum Peeling**. The FIB-54 experimental program (Appendix D) and finite element modeling (Appendix F) have shown that the maximum peeling stress along a given section occurs when only the outboard (closer to the outside edge) strands are cut. This condition is referred to as the "maximum peeling" condition.

- **Combined**. This condition occurs when strands along a given section are cut and Hoyer stresses are superimposed with peeling stress. It is referred to as the "combined" condition.

The model does not consider stress conditions when inboard (closer to the centerline) strands have been cut. FE modeling (Appendix F) has shown that cutting of inboard strands reduces peeling stresses at the end of a girder.

Figure 53–Flange splitting in experimental girder
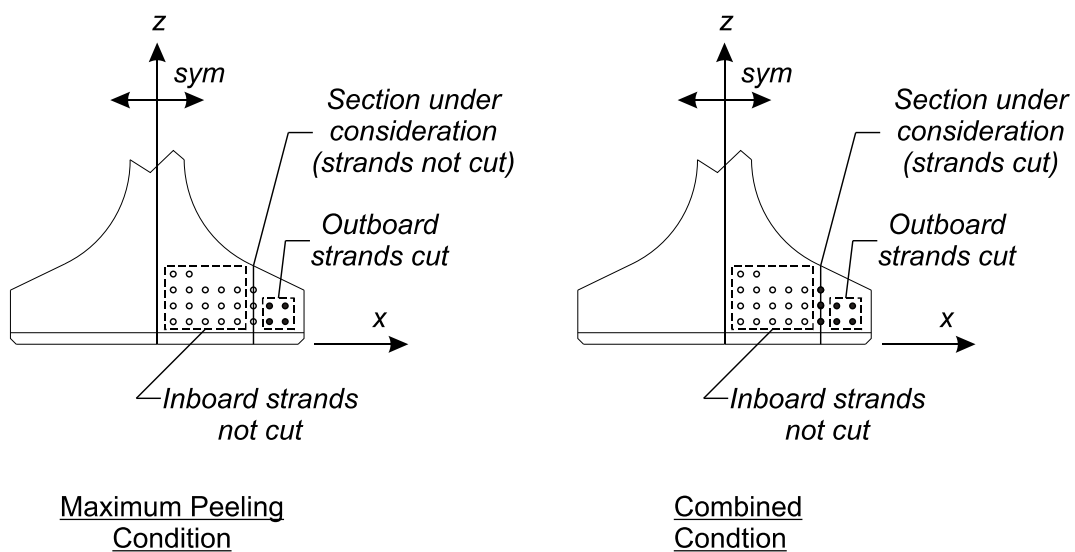
Figure 54–Strand release conditions

The serviceability model can be used to calculate average stress at the end of a girder along a vertical line through the flange. For FIB girders, the model can be used to calculate average stress at the member end along lines A through E as shown in Figure 55. The worst stress along any of these lines, and for either of the critical stress conditions (maximum peeling or combined), is the governing stress that should be used for comparison with the concrete tensile capacity.
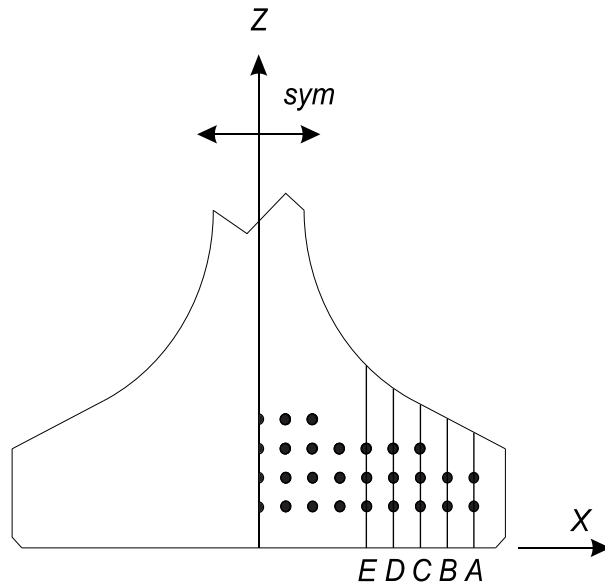
Figure 55–Analysis sections for FIB bottom flange

Peeling stress calculations are based on the free body diagram shown in Figure 56. This figure shows peeling stresses at the end of the member that result from an internal moment in the bottom flange. The internal moment is created by eccentricity between the applied prestressing force and the resultant axial force. Additional details and justification for this approach are given in Appendix G. Equation 8-5 was derived from the free body diagram and can be used for calculating peeling stresses at the end of a member.
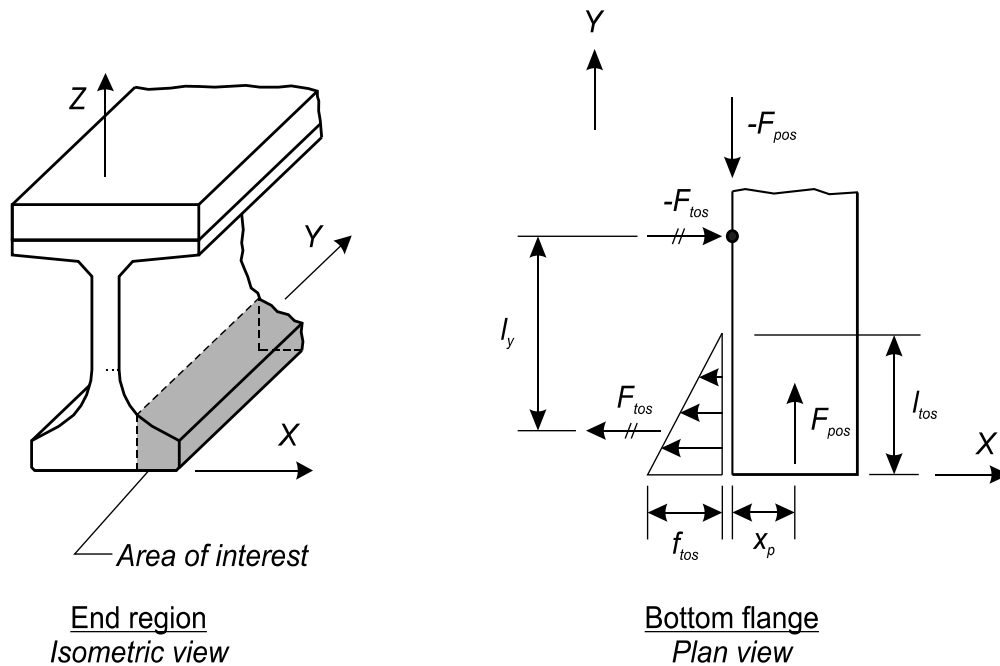
Figure 56–Bottom flange free body diagram

$$f_{tos} = \frac{2F_{pos}x_p}{l_y l_{tos}(h_f - n_{st}d_b)}$$

8-5

Where:

$f_{tos} =$ Peeling stress at location under consideration
$F_{pos} =$ Prestressing force from strands outboard of cut plane
$x_p =$ Distance from cut plane to centroid of prestressing force
$l_y =$ Internal moment arm in y-direction (see Appendix G for equations)
$l_{tos}=$ Length of the assumed tensile stress distribution
$n_{st} =$ Quantity of all strands along location under consideration
$d_b =$ Diameter of prestressing strands

Hoyer stress calculations are based on a model derived by Oh et al. (2006). The Oh model considers constitutive and geometric properties of steel and concrete as well as the level of prestressing. Building on the Oh model, Equation 8-6 was derived for calculating Hoyer stresses. Stress calculated by this equation is the average stress on a vertical line through the bottom flange at the end of a member. Stressing 0.6-in. diameter strands to 75% f_{pu} causes a 0.21% decrease in strand radius.

$$f_h = \frac{n_s \, d_b}{\left(h_f - n_{st}d_b\right)}\left[\frac{r_0 - r_j}{\left(1 - v_p\right)r_0/E_p + (v_c + 1)r_j/E_c}\right] \qquad \text{8-6}$$

Where:

$f_h =$ Average stress at location under consideration due to Hoyer Effect
$n_s =$ Quantity of fully bonded strands along location under consideration
$d_b =$ Diameter of prestressing strand
$h_f =$ Thickness of flange at location under consideration
$n_{st} =$ Quantity of all strands along location under consideration
$r_o =$ Strand radius before pretensioning
$r_j =$ Strand radius immediately after pretensioning
$v_p =$ Strand Poisson ratio
$E_p =$ Strand Elastic Modulus
$v_c =$ Concrete Poisson ratio
$E_c =$ Concrete Elastic Modulus

Stresses calculated using the serviceability model correlate well with flange crack data from the FIB-54 and FIB-63 test girders (Figure 57). This can be seen from the linear curve in Figure 57 that is fit to the stress and crack data. The line has an R^2 value of 0.85, indicating a high degree of correlation between calculated stresses and experimental crack lengths. Considering the random nature of cracking in concrete, this level of correlation suggests that the model does an excellent job of capturing the physical phenomenon which cause bottom flange splitting cracks.
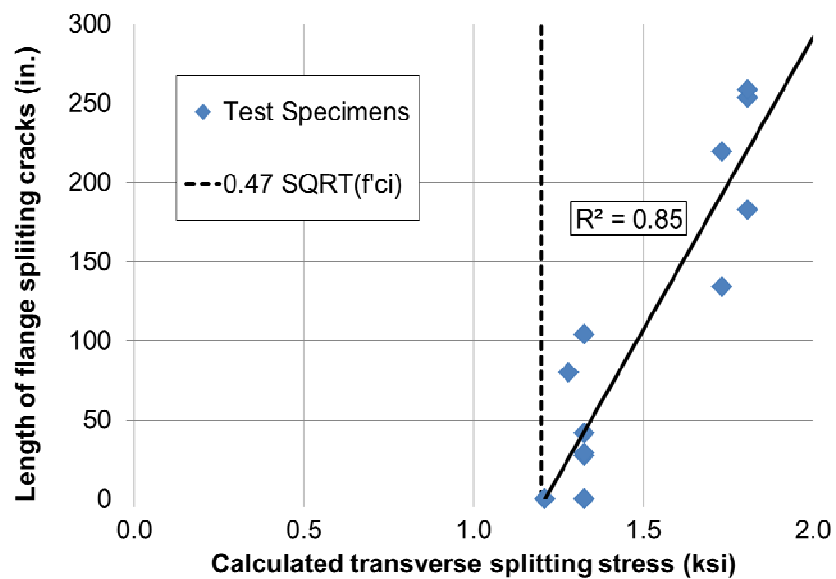
Figure 57–Calculated transverse splitting stress vs. experimental crack length

8.3 Ultimate Strength Design of Confinement Reinforcement

The ultimate strength model derived previously can be used for AASHTO LRFD design using 8-7:

$$\phi A_{CR} f_{yCR} = F_{CRu} \qquad 8\text{-}7$$

Where:

$A_{CR} =$ Required area of confinement reinforcement

$f_{yCR} =$ Yield stress of confinement reinforcement

$\phi =$ Resistance factor

The required area of confinement reinforcement is such that the confinement reinforcement must provide a design strength greater than the force generated by the strand anchorage or the transverse tie. The resistance factor should be determined using the AASHTO LRFD reliability analysis of the limit states. In lieu of this it is reasonable to treat this reinforcement the same as tension steel in an anchorage zone ($\phi = 1.0$).

8.4 Conclusions

Models were derived for designing confinement reinforcement and for calculating transverse tensile stresses in the bottom flange of I-girders. The confinement reinforcement model can be used to design confinement reinforcement to resist lateral-splitting failure at ultimate load. The tensile stress model can be used to determine the likelyhood of flange splitting cracks at the serviceability limit state. Both models were found to compare favorably with experimental data.

9   Recommendations

Based on the literature review, experimental, and analytical work detailed in this report, the following recommendations are made:

Load rating of lightly reinforced sections similar to SR-72 girders:

- The experimentally determined shear capacities should be considered when evaluating girders similar to the SR-72 test girders. Experimental capacities of interior girders were approximately 70% larger on average than capacities calculated by ACI 318 and AASHTO LRFD methods.
- Concrete shear contribution, as calculated by ACI 318 or AASHTO LRFD methods, are recommended for estimating the cracking load of girders similar to the SR-72 test girders. Concrete contribution as calculated by ACI 318 and AASHTO methods were, respectively, 17% and 32% lower than the experimental cracking loads.
- Strength contribution from integral curbs and barriers can be conservatively neglected when analyzing members similar to the SR-72 test girders. Should evaluations show that contribution of curbs is critical, it is noted that exterior girders with integral curbs had 30% greater shear capacity than similar interior girders without curbs. Test girders with curbs also exhibited increased stiffness over interior girders.
- Evaluations of members similar to the SR-72 test girders should consider the possibility of prestressing forces up to 50% lower than the specified prestress. The large difference between the specified and experimental values may indicate quality control issues in addition to higher than expected losses.

Confinement reinforcement and bearing plates in precast/pretensioned I-girders:

- The end region design procedures developed as part of this research provide a rational approach for designing confinement reinforcement for both service and strength conditions. Full scale testing and the end region design provisions indicate that the current FDOT confinement reinforcement is adequate for girders up to at least FIB-63. The current detail places #3 confinement reinforcement at 3.5-in. spacing over a distance approximately $0.3d$ from the member end and at 6-in. spacing over a distance approximately $1.5d$ from the end. The current detail also includes an embedded steel bearing plate at each member end.
- In special cases where additional bottom flange crack control or lateral-splitting capacity is required, #4 bars should be used for confinement reinforcement in lieu of the currently specified #3 bars. Such cases may include: girders with factored reaction forces larger than the experimental capacities from the test program, girders in aggressive environments wherein flange cracking is a critical durability concern, girders with partially bonded strands clustered below the web, and/or girders without embedded steel bearing plates.

- Embedded steel bearing plates performed well in the research program and are recommended for continued use. Bearing plates utilizing the current FDOT design standards improved the test girders with respect to serviceability and strength criteria.
- Use of longer studs on bearing plates is recommended for future research. It is believed that longer studs will engage a greater portion of concrete, thereby providing additional confinement to the bottom flange. Wider (in the direction of the span length) bearing plates are also recommended for future research. Wider bearing plates may prevent cracking near the member end, and thereby improve bond-shear capacity.

Strand and partial debonding patterns:

- Fully bonded strands should be placed as close to the cross-section centerline and with as much top cover as practical. This practice will reduce the likelihood of bottom flange splitting cracks forming and propagating during and following prestress transfer. In addition, the potential that lateral-splitting failure will control the shear strength will be reduced.
- Current AASHTO LRFD limits on termination of strand shielding at a given section are recommended for controlling flange splitting cracks within the transfer length of partially shielded strands. Confinement reinforcement is believed unnecessary at these locations if shielding termination complies with the AASHTO LRFD limits.
- Although further research is needed, this project has demonstrated that the percentage of shielded strands can reasonably exceed the 25% limit currently specified by AASHTO LRFD if sufficient reinforcement and strands are provided to meet minimum longitudinal steel requirements at the girder end. As currently specified by AASHTO LRFD, any lack of full development must be considered when evaluating the minimum longitudinal steel.
- Partially shielded strands (when used) should be placed towards the outside of the bottom flange. Clustering of shielded strands below the web is strongly discouraged.
- Prestress force in the outermost strands in the bottom two rows should be reduced from the currently specified level for the FIB sections. A prestress force of 10 kip is recommended in order to support reinforcement during fabrication. This practice will reduce the likelihood of bottom flange splitting cracks and lateral-splitting failure.

End region detailing to prevent/control lateral web splitting cracks:

- The current FDOT detail for vertical end region reinforcement is recommended for continued use. In spite of high stresses in the end region of the test specimens, the FDOT detail kept crack widths within the FDOT acceptance criteria for moderate environments.
- Strand shielding is recommended for use in controlling end region stresses and web splitting cracks. Negative effects of shielding on end region capacity and cracking load must be considered when utilizing strand shielding to control web cracks.
- The post-tensioning detail used in the FIB-63 test program is not recommended for use in its current form. Issues with this detail included cracks propagating from the post-tensioning bearing plate and vertical cracking from the end of the bottom flange due to development of the post-tensioning rods.
- Increasing the area of vertical reinforcement in the end region beyond the current FDOT level is recommended when circumstance warrant. The use of 1-in. diameter all-thread

rods is recommended as a means of increasing the area of vertical reinforcement. If used, heavy nuts should be placed top-and-bottom of the rods to aid in development. One option is to anchor bars by threading into tapped holes in bearing plate or nuts welded to top of plate surface.

- Horizontal reinforcement in the end region was omitted from FDOT standard details beginning with the 2010 interim design standard. The decision to omit horizontal reinforcement was validated by the experimental program. Experimental capacity of girders with and without horizontal end region reinforcement differed by a marginal 2%.

10 References

American Association of State Highway and Transportation Officials (2007), *AASHTO LRFD Bridge Design Specifications* 4th Edition." Washington, D.C.

American Association of State Highway and Transportation Officials (2010), *AASHTO LRFD Bridge Design Specifications* 5th Edition." Washington, D.C.

ACI (2008), *Building Code Requirements for Structural Concrete and Commentary ACI 318-08*, American Concrete Institute, Farmington Hills, MI.

ACI (2011), *Building Code Requirements for Structural Concrete and Commentary ACI 318-11*, American Concrete Institute, Farmington Hills, MI.

ADINA R&D Inc. (2009), ADINA version 8.6. Watertown, MA.

Aknoukh, A. (2010), "The Effect of Confinement on Transfer and Development Length of 0.7 Inch Prestressing Strands," Concrete Bridge Conference. Phoenix, AZ.

ASCE-ACI Task Committee 426. (1973), "The Shear Strength of Reinforced Concrete Members." *Journal of the Structural Division*, 99(6), pp. 1091-1187.

Barnes, R., Burns, N., and Kreger, M. (1999), *Development Length of 0.6-Inch Prestressing Strand in Standard I-Shaped Pretensioned Concrete Beams* Rep. No. 1388-1, Texas Department of Transportation, Austin, TX.

Breen, J., Burdet, C., Sanders, D., and Wollmann, G. (1991), *Anchorage Zone Reinforcement for Post-Tensioned Concrete Girders,* National Highway Cooperative Research Program. Transportation Research Board. Washington, D.C.

Castrodale, R.W., Lui, A., and White, C.D. (2002), "Simplified Analysis of Web Splitting in Pretensioned Concrete Girders." *Proceedings, PCI/FHWA/NCBC Concrete Bridge Conference*, Nashville, TN, October 6-9.

CEB-FIP (1993), *International Recommendations for the Design and Construction of Concrete Structures,* Comité Euro-International du Béton, Thomas Telford, London.

Chong, O. and Arthur, P. (1987), "Ultimate Strength of Uniformly Loaded Reinforced Concrete T-Beams." *Structural Engineer, Part B: R&D Quarterly*, 65B(1), pp 10.

Consolazio, G., Fung, J., and Ansley, M. (2004), "M-ϕ-P Diagrams for Concrete Sections Under Biaxial Flexure and Axial Compression," *ACI Struct.J*, 101(1), pp 114-123.

Cook, R. and Reponen, M. (2008), *Prevention of Splitting Failure at the Ends of Prestressed Beams during Fabrication,* Rep. No. BD545-30. Florida Department of Transportation, Tallahassee, FL.

Crispino, E.D. (2007), *Anchorage Zone Design for Pretensioned Bulb-Tee Bridge Girders in Virginia*, Thesis, Virginia Polytechnic Institute and State University, Blacksburg, VA, 155 pp.

Csagoly, P. (1991), *A Shear Moment Model for Prestressed Concrete Beams,* Rep. No. 9900-1550, Florida Department of Transportation, Tallahassee, FL.

Davis, R.T., Buckner, C.D., and Ozyildirim, C. (2005), "Serviceability-Based Design Method for Vertical Beam End Reinforcement," *Proceedings of PCI National Bridge Conference*, Palm Springs, CA, 16-19 Oct 2005.

Deatherage, J., Burdette, E., and Chew, C. (1994), "Development Length and Lateral Spacing Requirements of Prestressing Strands for Prestressed Concrete Bridge Girders, *PCI Journal*. Jan-Feb, pp. 70-83.

Dunkman, D. (2009), "Bursting and Spalling in Pretensioned U-Beams," thesis. University of Texas, Austin.

Englekirk, R. E. and Beres, A. (1994), "Need to develop shear ductility in prestressed members," *Concr.Int*, 16(10), 49-56.

Fallaha, S. (2009). Telephone and E-mail correspondence with Brandon Ross.

FHWA (2010), "Federal Highway Administration National Bridge Inventory," http://www.fhwa.dot.gov/bridge/nbi/mat09.cfm (accessed December 1, 2010).

Florida Department of Transportation (FDOT) (2008), *Interim Design Standard Index No. 20054,* Florida Department of Transportation, Tallahassee, FL.

FDOT (2009), *Structures Design Guidelines*, Tallahassee, FL.

FDOT (2009a), *Temporary Design Bulletin C09-01,* Tallahassee, FL.

FDOT (2009b), *Temporary Design Bulletin C09-03*, Tallahassee, FL.

FDOT (2009d), *Interim Design Standard Index No. 20510*, Tallahassee, FL.

FDOT (2010), *Interim Design Standard Index No. 20063A*, Tallahassee, FL.

FDOT (2012), *Specification 450 Precast Prestressed Concrete Construction*, Tallahassee, FL.

Gergely, P., Sozen, M.A., and Siess, C.P. (1963), *The Effect of Reinforcement on Anchorage Zone Cracks in Prestressed Concrete Members*, University of Illinois Structural Research Series No. 271, 170 pp.

Giaccio, C., Al-Mahaidi, R., and Taplin, G. (2002), "Experimental study on the effect of flange geometry on the shear strength of point loaded RC T-beams." *Canadian Journal of Civil Engineering*. 29(6) pp. 911-918.

Guyon, Y. (1955), *Prestressed Concrete* 2nd ed. (English translation), F.J. Parsons, London, 543 pp.

Harries, K.A. 2009, "Structural Testing of Prestressed Concrete Girders from the Lake View Drive Bridge," *ASCE Journal of Bridge Engineering*, 14(2), pp 78-92.

Hoyer, E. (1939), *Der Stahlsaitenbeton*, Otto Elsner, Berlin.

Ibell, T., Morley, C., and Middleton, C., (1999), "Strength and behaviour in shear of concrete beam-and-slab bridges," *ACI Struct.J*, 96 (3), pp. 386-391.

Iyengar, K. (1962), "Two-Dimensional Theories of Anchorage Zone Stresses in Post-Tensioned Prestressed Beams," *ACI Journal*, 59(10), pp. 1443-1466.

Kannel, J., French, C., and Stolarski, H., (1997), "Release Methodology of Strands to Reduce End Cracking in Pretensioned Concrete Girders," *PCI Journal,* 42(1), Jan.–Feb., pp. 42–54.

Kotsovos, M., Bobrowski, J., and Eibl, J., (1987), "Behavior of Reinforced Concrete T-Beams in Shear," *Structural Engineer, Part B: R&D Quarterly*, 65B(1), pp1-10, March.

Kaufman, M. K. and Ramirez, J. A. (1988), "Re-Evaluation of the Ultimate Strength Behvaior of High-Strength Concrete Prestressed I-Beams," *ACI Struct.J*, 85(3), 295-303.

Kuchma, D., Kim, K. S., Nagle, T. J., Sun, S., and Hawkins, N. M. (2008), "Shear tests on high-strength prestressed bulb-tee girders: Strengths and key observations," *ACI Struct.J*, 105(3), 358-367.

Leonhardt, F., Walter, R. (1962), *The Stuttgart Shear Tests 1961*, Translation III. Cement and Concrete Association Library. London.

Leonhardt, F. and Walther, R, (1961), "The Stuttgart Shear Tests," *Benton -und Stahlbetonbau*, 56(12) and 57(2,3,6,7, and 8), Translation by Amerongen, C.

Llanos, G., Ross, B., and Hamilton, H. (2009). "Shear Performance of Existing Prestressed Concrete Bridge Girders." Rep. No. BD 545-56, Florida Department of Transportation, Tallahassee, FL.

Magus, R. (2010). Brandon Ross notes from pre-construction meeting. Dura-Stress, Leesburg, FL.

Marshall, W. and Mattock, A. (1962), "Control of Horizontal Cracking in the Ends of Pretensioned Prestressed Concrete Girders," *PCI Journal*, 7(10), pp. 56-75.

Maruyama, K. and Rizkalla, S. H. (1988). "Shear Design Consideration for Pretensioned Prestressed Beams," *ACI Struct.J*, 85(5), 492-498.

Morcous, G., Hanna, K., and Tadros, M., (2010), *Bottom Flange Reinforcement in NU I-Girders*, Nebraska Department of Roads, Lincoln, NE.

Nolan, S. (2009). Telephone and E-mail correspondence with Brandon Ross.

North American Strand Producers Association (NASP) (2009), "Standard Test for Strand Bond"

Patzlaff, Q., Morcous, G., Hanna, K., and Tadros, M., (2010), "Bottom Flange Reinforcement of Precast-Prestressed Bridge I-Girders," 2010 Concrete Bridge Conference.

Oh B., Kim K., and Lew Y., (2002), "Ultimate Load Behavior of Post-Tensioned Prestressed Concrete Girder Bridge through In-Place Failure Test," *ACI Struct J*, V. 99, No. 2, March-April.

Oh, B., Kim E., and Choi Y., (2006), "Theoretical Analysis of Transfer Lengths in Pretensioned Prestressed Concrete Members." *ASCE J of Engineering Mechanics*, October.

O'Neill, C. and Hamilton, H. (2009), *Determination of Service Stresses in Pretensioned Beams*, Rep. No. BD 545-78, Florida Department of Transportation. Tallahassee, FL.

PCI (1999), *PCI Design Handbook*. 5th ed. Chicago, IL

Pessiki, S., Kaczinski, M., and Wescott, H., (1996), "Evaluation of Effective Prestress Force in 28-Year-Old Prestressed Concrete Bridge Beams," *PCI Journal*, v 41, n 6, pp 78-89, Nov-Dec.

Placas, A. and Regan, P., (1971), "Shear Failure of Reinforced Concrete Beams," *ACI J*, October, pp. 763-773.

Ritter, W. (1899), "Die Bauweise Hennebique," *Schweizerische Bauzeitung,* Zurich, February.

Roberts, C. (1990), *Behavior and Design of Local Anchorage Zone of Post-Tensioned Concrete Members*, M.S. Thesis. University of Texas. Austin, TX.

Ross, B., Ansley, M., and Hamilton, H., (2011), "Load Testing of 30-year-old AASHTO Type III Highway Bridge Girders," *PCI Journal*, 56(4), 152-163.

Russell, B. and Burns, N. (1996), "Measured Transfer Lengths of 0.5 and 0.6 in. Strands in Pretensioned Concrete," *PCI Journal*, Sept.-Oct., pp. 44-54.

Ruddle, M., Rankin, G., and Long, A., (2003), "Arching Action – Flexural and Shear Strength Enhancements in Rectangular and Tee Beams," *Proceedings of the ICE – Structures and Buildings*, 156(1), February, pp. 63-74.

Schlaich, J., Schäfer, K., and Jennewein, M. (1987), "Toward a Consistent Design of Structural Concrete," *PCI Journal*, 32(3), pp. 74-150.

Shahawy, M., Robinson, B., and deV Batchelor, B. (1993), "An Investigation of Shear Strength of Prestressed Concrete AASHTO Type II Girders," Florida Department of Transportation, Tallahassee, FL.

Tadros, M., Badie, S., and Tuan, C. (2010), "Evaluation and Repair Procedures for Precast/Prestressed Concrete Girders with Longitudinal Cracking in the Web," National Cooperative Highway Research Program, Report 654, Transportation Research Board, Washington, D.C.

Tuan, C., Yehia, S., Jongpitakseel, N., and Tadros, M., (2004), "End Zone Reinforcement for Pretensioned Concrete Girders," *PCI Journal*, Vol. 49, No. 3, pp. 68-82.

Yura, J., Kumar, A., Yakut A., Topkaya, C., Becker, E. and Collingwood, J., (2001), *Elastomeric Bearing Pads: Recommend Test Methods*," National Cooperative Highway Research Program Report 449, Transportation Research Board, Washington, D.C.

Zararis, I., Karaveziroglou, M., and Zararis, P., (2006), "Shear strength of reinforced concrete T-beams," *ACI Struct.J*, Vol. 103, No. 5, pp. 693-700.

Appendix A–Literature Review

Appendix B−Small Beam Tests

Appendix C—SR-72 Tests

Appendix D–FIB-54 Tests

Appendix E–FIB-63 Tests

Appendix F–Finite Element Analysis of End Region

Appendix G–End Region Design Models

Appendix H–Support Data